GROWTH AND ECOPHYSIOLOGICAL RESPONSES OF FRASER FIR (*Abies fraseri*) CHRISTMAS TREES ALONG AN ELEVATIONAL GRADIENT

A Thesis
by
SCOTT THOMAS CORY

Submitted to the Graduate School
at Appalachian State University
in partial fulfillment of the requirements for the degree of
MASTER OF SCIENCE

December 2015
Department of Biology

GROWTH AND ECOPHYSIOLOGICAL RESPONSES OF FRASER FIR (*Abies fraseri*) CHRISTMAS TREES ALONG AN ELEVATIONAL GRADIENT

A Thesis
by
SCOTT THOMAS CORY
December 2015

APPROVED BY:

_____
Howard S. Neufeld
Chairperson, Thesis Committee

_____
Michael D. Madritch
Member, Thesis Committee

_____
Keith Reinhardt
Member, Thesis Committee

_____
Zack E. Murrell
Chairperson, Department of Biology

_____
Max C. Poole
Dean, Cratis Williams Graduate School

Abstract

GROWTH AND ECOPHYSIOLOGICAL RESPONSES OF FRASER FIR (*Abies fraseri*) ACROSS AN ELEVATIONAL GRADIENT

Scott Cory
B.S., University of North Carolina at Chapel Hill
M.S., Appalachian State University

Chairperson: Dr. Howard S. Neufeld

Fraser fir (*Abies fraseri)* Christmas tree production is a $100 million dollar/year industry in North Carolina, but the future of these trees may be threatened by predicted global climate change. To evaluate how this species will respond to climate drivers associated with warming, I studied growth and ecophysiology of Fraser fir Christmas trees along an elevational gradient from 664 to 1228 m. Daytime maximum temperatures and evaporative demand were highest at low elevation and cloud events occurred more often at high elevations. Architectural characteristics such as specific needle mass, needle packing density, and silhouette-to-projected area ratios generally did not vary along the elevational gradient. Bud-burst occurred 6 days sooner, new shoots ceased elongation 10 days sooner, and radial trunk growth ended 8 days later at low elevations than at high elevations, indicating a lengthening of the growing season. However, total % increase in trunk diameter was greatest at middle elevations. Gas exchange at the needle level was measured under standard conditions using the Li-6400xt portable gas exchange system, which showed that the capacity for photosynthesis did not decrease with elevation, but did as needles aged.

Diurnal patterns of gas exchange under ambient conditions at the shoot level were measured 3 times during the 2014 growing season and showed that rates of photosynthesis tended to peak earlier in the morning at low elevations, and later at higher elevations. When diurnal measurements of photosynthesis were integrated over the three days of measurement at each elevation they showed that daily carbon gain was lowest at low elevations, and that this resulted primarily from low rates early in the season, when temperatures rose above 30°C at this site. As climate change progresses, higher cloud ceilings, increased evaporative demand, and higher temperatures will further reduce growth and ecophysiological functioning at low elevation Christmas tree farms, but middle and high elevation farms may benefit from a longer growing season.

Acknowledgements

I would like to acknowledge my advisor, Dr. Howard Neufeld, for all of his support, wisdom, and assistance throughout this project. Thanks to Dr. Michael Madritch for his assistance with C:N analyses and Dr. Keith Reinhardt for his advice on techniques for measuring gas exchange of conifers. This research was completed through close collaboration with Lauren Wood, and I would like to thank her for assistance with forming hypotheses, designing experiments, and planning and executing our field work. Additionally, this project would not have been possible without the support of Dr. Jim Hamilton and Jeff Owen from the North Carolina Cooperative Extension Service, who helped us choose appropriate field sites and contact Christmas tree growers. Funding was provided by the Cratis D. Williams Graduate School and Office of Student Research at Appalachian State University. Lastly, I appreciate the cooperation of all the growers: Carroll Garland, Sr., Ronnie Duckworth, Thad Taylor, Burl Greene, Jim Bryan, and Danny Miller.

Dedication

To my late grandfather, Joe Klimek. I fondly remember our trips to botanical gardens, the Norway spruce and Dawn Redwood in his back yard, and the way he loved seeing fall colors in the mountains.

My grandfather and I, circa 2008

Table of Contents

Foreword

This research was done in close collaboration with Lauren Wood, as part of a comprehensive study of growth, phenology, carbon relations, and water relations of Fraser fir Christmas trees. Our work will be combined for publications. References are in the style of the journal *Tree Physiology*.

Introduction

Fraser firs (*Abies fraseri* [Pursh] Poir.) occur naturally on seven high-elevation peaks above 1500 m and occupy ~18000 ha in the southern Appalachian Mountains, where they experience frequent cloud immersion and cool temperatures during the growing season (Johnson and Smith 2006, Potter et al. 2008, Berry and Smith 2013, Berry et al. 2013). Survival of Fraser fir in this habitat is likely due to these unique microclimatic conditions. Here, daytime temperatures rarely exceed 22 °C and trees experience cloud immersion at some time during the day on ~70% of all days (Reinhardt and Smith 2008a, b, Berry and Smith 2012). These cool temperatures and cloud conditions improve plant water status by reducing leaf-to-air water vapor pressure deficit (VPD) and by maintaining high soil moisture content, and hence plant water uptake, via droplets that condense directly on the ground or on plant surfaces. Additionally, Berry and Smith (2014) showed that Fraser firs are capable of direct foliar uptake from cloudwater. Studies using isotopes of H and O have shown that clouds can account for ~30% of plant water uptake for Fraser firs at these high-elevation peaks (Berry et al. 2013, 2014).

Although Fraser firs in their native range (>1500 m) are adapted to these unique microclimatic conditions, this species is grown commercially as Christmas trees at much lower elevations (as low as 600 m). Fraser fir is overwhelmingly the most popular species of Christmas tree in the southern Appalachians, accounting for over 90% of commercial production. In North Carolina alone, ~50 million trees are growing on >30,000 ha, and the industry is valued at >$100 million/year (NC Cooperative Extension Service, 2015). Grown from native population seed sources, Christmas trees at these lower elevation farms are genetically derived from to trees growing at their natural, high-elevation locations (Arnold et

al. 1994, Emerson et al. 2006, 2008), but they require both weeding to eliminate competition from other vegetation and a variety of fungicides and pesticides to reduce fungal pathogens and pests that they are exposed to at these lower elevations which they do not encounter in their natural ranges. Moreover, in the locations of these lower-elevation farms, they experience very different microclimate and environmental stressors than in their native range, including higher temperatures, increased evaporative demand, lower soil moisture, and less frequent cloud immersion. Due to these elevationally-based stressors, Christmas trees grow in a very different radiation climate as well a warmer, drier one, and operate at a reduced water budget compared to their native counterparts**.**

These elevationally based stressors are similar to predications about how climate will change due to global warming (Reinhardt et al. 2011, King et al. 2013); therefore, the elevational gradient over which commercial Fraser firs are grown can serve to some extent as a surrogate for climate warming (i.e., a "space for time" substitution), enabling us to study how this species may respond to future climate change. Other ecologists have used the 'elevation as surrogate for warming' experimental approach to assess the effects of temperature on ecophysiological functioning (Fryer and Ledig 1972, Richardson and Berlyn 2002, Reinhardt et al. 2011, Wertin et al. 2012), leaf morphology (Cordell et al. 1998, Richardson et al. 2001, Poulos and Berlyn 2007), phenology (Royce and Barbour 2001, Vitasse et al. 2013), and growth (King et al. 2013, Sidor et al. 2015) for a variety of other tree and herbaceous species. No previous research has specifically investigated these characteristics using an elevational gradient as a proxy for climate warming in Fraser fir Christmas trees. Although Fraser fir Christmas trees survive and grow adequately at low elevations until harvest age (~11-14 years), indicating a tolerance of current water stress and

high temperatures, the degree of stress in these habitats may become more significant as climate warming progresses. Furthermore, there have been no physiological studies performed to inform Christmas tree growers about what the ideal elevations are for growing Christmas trees under both current and future climates.

Evidence of climate warming in the southeastern United States, and particularly in the Southern Appalachians, is somewhat conflicting. Laseter et al. (2012) found that since the early 1980s, mean annual temperatures at Coweeta Hydrologic Laboratory in the mountains southeast of Great Smoky Mountains National Park have increased by 0.5 °C per decade, and that precipitation is becoming more variable among years. On Grandfather Mountain, minimum and mean temperatures and heating degree-days have also increased from 1956 to 2007 (Soulé 2011). However, Warren and Bradford (2010) found that, during the period 1931-2004, temperatures were more variable among years, but were not increasing on average in this region. NOAA has also reported a lack of warming trends, but has documented an increase in inter-annual variability in precipitation for the period 1895-2011 in the Southeast U.S. (Kunkel et al. 2013). Similarly, Zhang et al. (2007) documented a lack of a warming and precipitation trends in Great Smoky Mountains National Park during the period 1971-2001, and they also describe analogous inter-annual fluctuation.

Additionally, cloud ceilings are expected to rise and cloud events will occur less often as climate change progresses (Richardson et al. 2003, IPCC 2013, Kunkel et al. 2013), which may be particularly important for Fraser firs. In fact, rising cloud ceilings have already been observed in the southern Appalachians; during the period from 1973-1999; cloud ceilings were at ~1071 m in 1999 but are rising at a rate of 8.8 ± 0.3 m yr^{-1} (mean ± s.e.) (Richardson et al. 2003). Although some high elevation Christmas tree farms are located above this

ceiling, if the cloud ceiling continues to rise at this rate, then even the highest elevation farms (~1400 m) will be below it by 2036.

The ecophysiology of Fraser firs in their native range has been documented to some degree, but only a few studies have focused on the ecophysiology of Christmas trees. This research has focused mainly on improving commercial production and on agricultural practices such as shearing techniques, fertilization regimes, and spacing (Hinesley and Wright 1989; Hinesely and Snelling 1997; Hinesley and Derby 2004), as well as on genetic characteristics (Arnold et al. 1994; Emerson et al. 2006, 2008), and pest management (Liesch and Williamson 2010, Richter et al. 2011). Although this research is useful for the industry for increasing the economic value of Christmas trees, we do not have a very good understanding of the environmental factors limiting gas exchange and growth for commercially grown Fraser fir trees. The few ecophysiological studies that have been done on these trees used 3-year-old containerized seedlings in greenhouses. For example, Kulaç et al. (2012) exposed containerized Fraser fir seedlings to drought and found significant increases in chlorophyll fluorescence and reductions in concentrations of photosynthetic pigments. Additionally, Nzokou and Cregg (2010a, 2010b) demonstrated that both nitrogen and water availability limit growth in containerized seedlings, and that nitrogen fertilization can buffer the negative effects of drought stress by causing re-allocation of resources to root development. This may partly explain the survival of Fraser fir Christmas trees at lower elevation farms. Although these in situ trees are not irrigated, they do receive ample nitrogen fertilization, which may help them cope with the drought stress at lower elevations by increasing root mass to explore a larger volume of soil. However, ~12-year-old in situ trees

may function quite differently than containerized seedlings in a greenhouse, so the ecophysiological responses of in situ small trees vs. containerized seedlings remains unclear.

In this study, I monitored the timing and magnitude of growth, photosynthetic carbon relations, and plasticity and adjustments of leaf and shoot architecture along an elevational gradient from 664 m to 1228 m, which I used as a surrogate for future climate warming (Fig. 1). No previous research has specifically investigated these characteristics in Fraser fir Christmas tree farms along an elevational gradient. My research addressed the following three hypotheses: (H1) In response to elevationally-based stressors, these trees may extend their growing season, resulting in earlier bud-break and foliar growth and later cessation of cambial growth. If trees at low elevations advance their bud-break phenology, it would indicate that bud-break is cued primarily by spring temperatures rather than photoperiod or prior exposure to winter chilling (Körner and Basler 2010, Basler and Körner 2012). (H2) Mid-summer high temperatures and increased water stress at lower elevations will result in decreased rates of carbon assimilation compared to trees at higher elevations (at seasonal time scales). As a corollary, I also predicted that trees at higher elevations have higher nutrient contents (specifically N) due to less growth dilution because of a shorter growing season and lower temperatures, and also because ambient N deposition rates tend to increase with elevation (Nodvin et al. 1995). (H3) To cope with higher temperatures and water stress, shoot-level architecture may adjust to maximize self-shading at the hottest and driest times of day, and needle-level architecture and morphology will change to minimize evaporative demand by decreasing total surface area from which water can evaporate. Although plasticity in these traits has been demonstrated in other species in their native ranges (Smith and Carter

1988, Witkowski and Lamont 1991, Boyce 1993, Poulos and Berlyn 2007), it has not yet been investigated in Fraser firs.

Methods

Study Sites

Prior to the 2014 growing season, six Christmas tree farms ranging from 664 to 1228 m were chosen for study in collaboration with the North Carolina Cooperative Extension Service (Table 1), with the premise that elevation could be used as a surrogate for warming. In order to minimize factors that could be confounded with elevation, study sites had similarly aged trees (~11-14 years old, 2.5 ± 0.2 m tall) that originated from common seed sources among all farms, were planted at near equivalent densities (3906 ± 152 trees/ha; mean ± se; 5 of 6 farms in 99% confidence interval), and were located on N-facing slopes. Farmers at each site practiced similar agriculture techniques in terms of trimming and fertilization, although our sample trees were not trimmed during the two years we studied them. At each farm, 10 trees were selected for study and each was located at least 3 m from another, but all were within a 15 m radius, in order to preserve independence among replicates while minimizing within-site variation.

Table 1. Location and characteristics of the study sites. Bold represents the site at each elevation category where weather stations were installed and gas exchange measurements took place. Predicted lapse at the low and middle elevation sites are the expected increase in daily maximum and minimum temperatures compared to high elevation sites, based on moist adiabatic lapse of 7 and 3 °C/km for daily maximum and minimum temperatures, respectively, reported by Bolstad et al. (1998) for the southern Appalachian Mountains. Tree heights are means ± s.e.

Site Name	Elevation (m)	Predicted T_{max} Lapse (°C)	Predicted T_{min} Lapse (°C)	Elevation Category	Geographical Coordinates	County, State	Tree Height (m)	Planting Density (# trees per ha)
Carroll1	664	3.9	1.7	Low	36°22'0.95"N 82° 0'54.47"W	Johnson, TN	2.38 ± 0.07	4499
Carroll2	**710**	**3.6**	**1.6**	**Low**	**36°23'3.37"N 81°51'19.69"W**	**Johnson, TN**	**2.62 ± 0.06**	**3660**
Thad	**1021**	**1.4**	**0.6**	**Middle**	**36°10'42.10"N 81°45'37.76"W**	**Watauga, NC**	**2.28 ± 0.04**	**4026**
Ronnie	1048	1.3	0.5	Middle	36°10'47.10"N 81°45'44.17"W	Watauga, NC	2.49 ± 0.06	3681
Jim	**1224**	**-**	**-**	**High**	**36°17'23.86"N 81°40'55.92"W**	**Watauga, NC**	**2.36 ± 0.04**	**4090**
Greene	1228	-	-	High	36°16'13.51"N 81°44'3.41"W	Watauga, NC	2.59 ± 0.07	3477

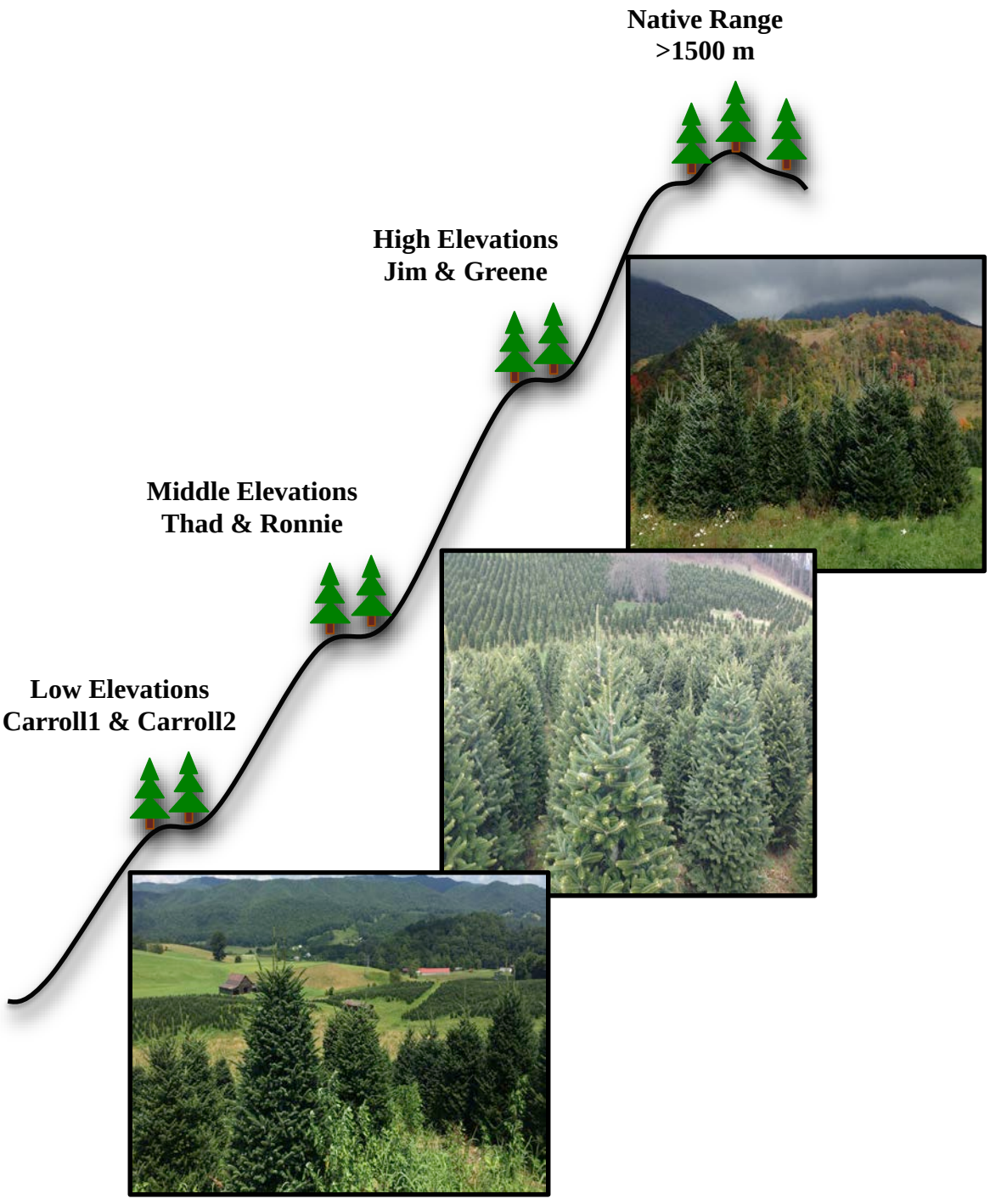

Figure 1. Schematic representation of study sites (see Table 1 for elevations of each site) and images of the study sites along with the names of each farm at each elevation category where weather stations were located and where gas exchange measurements took place.

Microclimate

Microclimatic conditions along the elevational gradient were monitored with Davis VantagePro2 weather stations (Davis Instruments, Hayward, California) installed in May 2014 at one site at each of the three main elevation categories (for which locations, see Table 1; images in Fig. 1). Weather stations were centrally located amongst the study trees at a height of ~2 m. At each site, air temperature, relative humidity, precipitation, wind speed, and solar radiation were measured every 2 seconds and averages recorded every 10 minutes. Temperatures were expected to increase as elevation decreased due to the adiabatic lapse. Bolstad et al. (1998) reported an increase of 7 °C per 1000 m decrease in elevation for the daily maximum, and 3 °C per 1000 m decrease for the daily minimum temperatures in the southern Appalachian Mountains. Throughout each day, solar radiation and VPD (leaf-to-air water vapor pressure deficit) were integrated, yielding daily total insolation and evaporative demand.

Soil moisture was measured weekly at a depth of 0-20 cm from April to October, using a Campbell Scientific HydroSense II soil moisture probe (Campbell Scientific Inc., Logan, Utah). Three equally spaced measurements were made around each tree.

Bud, shoot, and trunk phenology

Bud-burst phenology was tracked to determine if warming affects the timing of release from dormancy and progression towards complete bud-burst. Beginning in April 2014, phenology was recorded weekly on 3 terminal buds, on each of 3 south-facing branches at breast height for each of the 10 study trees (9 buds per tree) at all 6 sites (540 buds total), based on 7 stages of bud-burst described and imaged by the North Carolina

Cooperative Extension Service. Stage 1 represented dormant, waxy buds, and stage 7 represented fully emerged green shoots (see Appendix I for images and descriptions of each stage). The dates that buds reached phenological stages 4 and 7 and the duration of bud expansion were calculated using 4-parameter models (Appendix Table I) fit to phenology trends of each tree individually using Sigmaplot 13.0 (Systat Software Inc., Point Richmond, CA).

After all buds emerged, the length of each new shoot was recorded weekly until shoots had ceased elongation to determine if timing, duration, and magnitude of shoot growth was affected by elevation. The dates that shoots reached 75 % and 95 % of their final lengths were calculated using 3-parameter models (Appendix Table II) fit to each tree individually using SigmaPlot 13.0. The duration of shoot elongation represents the time between phenological stage 7 and 95 % of total shoot length for each tree.

Timing and magnitude of trunk diameter growth was monitored by installing plastic dendrometer bands in March 2014 at 30 ± 10 cm above the soil, and cumulative circumferential growth was measured weekly from May to October by bending a flexible ruler around the trunk and measuring the increase in growth from a fixed point. Dendrometer bands were constructed according to the Global Forest Carbon Research Initiative protocols (http://www.ctfs.si.edu, accessed February 2014). Since trunk circumference at the beginning of the growing season varied slightly among trees and among sites, trunk growth of each tree was expressed as the percent increase in diameter relative to the starting spring diameter. The dates that trunks reached 50 % and 95 % of their total increase in diameter, and the duration of trunk growth, were calculated using 3-parameter models (Appendix Table III) fit to each tree individually using Sigmaplot 13.0.

Gas Exchange under Standard Conditions

Gas exchange was measured under standard conditions in order to determine the photosynthetic capacity of trees from the three elevations when environmental factors were controlled. These measurements were made on August 7th and 13th 2014 using a Li-Cor 6400xt portable gas exchange system (Li-Cor, Inc., Lincoln, NE) equipped with an LED illuminated chamber (6400-02B) on needles that formed during the current growing season (hereafter: Y0), the previous growing season (Y1), and two years previously (Y2), from one south-facing branch at breast height on each of 5 trees, at the sites containing the weather stations (see Table 1). Approximately 48 hrs prior to the gas exchange measurements, needles were trimmed such that a planar row of 6-8 needles would fit into the leaf chamber without significant self-shading and to eliminate the possibility of adjacent needles causing leaks. Additional experiments (not shown here) confirmed that gas exchange of needles being measured was not affected by removing these adjacent needles. Standard chamber conditions were: flow rate at 400 μmol s^{-1}, 400 μmol mol^{-1} CO_2, relative humidity (RH) within 5% of ambient (~70 % RH), and temperature 23 ± 1 °C. Net photosynthesis (A_{net}) was measured first at a PPFD of 1500 μmol m^{-2} s^{-1}, then dark respiration (R_d) at 0 PPFD. Afterwards, sample needles were removed from their stems and projected needle area was determined by laying needles on a flatbed scanner (CanoScan 9000F Mark II scanner, Canon USA, Melville, NY), removing image artifacts such as shadows and dust with Adobe Photoshop CC 2014 (Adobe Systems Inc., San Jose, CA), and then converting pixels from these jpg images to area in cm^2 using Black Spot, a shareware program (Varma and Osuri 2013). Accuracy of these needle area measurements was confirmed by scanning a NIST standard area disk (10-cm^2 steel disk), which yielded measurement errors < 0.5%.

Gas Exchange under Ambient Conditions

Diurnal patterns of gas exchange were measured three times at each of three sites across the elevational range throughout the growing season, using the LI-Cor 6400xt, but this time equipped with the conifer chamber (6400-05) and using ambient sunlight conditions, on 3 needle ages (Y0, Y1, Y2) on one south-facing branch from each of 5 trees, at the sites with the weather stations. The first gas exchange campaign occurred on June 2nd, 8th, and 18th, the second campaign on July 23rd, 25th, and 29th, and the third campaign on October 2nd, 4th, 9th, and 20th 2014. Approximately 48 hrs prior to the gas exchange measurements, needles were removed from their stems such that a 3-cm segment of intact needles would fit inside the conifer chamber, but adjacent needles would not cause leaks beneath the foam gaskets. Measurements began predawn (~5:00 am local time) and continued until dusk (~8:30 pm local time). During measurements, branches were retained in their original orientations, flow rate was 400-500 μmol s^{-1}, and conditions inside the chamber were maintained at ambient temperature, 400 μmol mol^{-1} CO_2 (sample), and within 5% of ambient RH. During the first campaign (June 2014), gas exchange was measured on Y1 and Y2 shoots, as Y0 shoots had not yet fully expanded. In the following 2 campaigns (July and October), Y0 shoots were also included. On July 10th and 11th of the following year (2015), gas exchange measurements were made using the same experimental setup, although only at mid-day rather than throughout the day, and needles were not trimmed prior to inserting branches in the chamber. Gas exchange fluxes were expressed on projected leaf area basis.

Silhouette to Single-Sided Projected Leaf Area Determination

During diurnal gas exchange measurements of each shoot, azimuth (degrees clockwise from true north) and inclination (degrees from horizontal) were recorded in the field. Then each stem segment was collected and brought to the laboratory, where it was mounted on a ring stand in its *in vivo* orientation. The NOAA Solar Calculator (esrl.noaa.gov/gmd/grad/solcalc/) was used to determine azimuth and elevation (degrees from true north and above horizontal, respectively) of the sun at the time of each gas exchange measurement made in the field. Then, a digital camera with a 200 mm equivalent lens was mounted at the various solar coordinates and shoots were photographed to obtain a silhouette image, which represented the surface area intercepting direct beam radiation during each diurnal gas exchange measurement. Stems were digitally removed from images using Adobe Photoshop CC 2014 (Adobe Systems Inc., San Jose, CA), so that only needles remained in the silhouette images. The Black Spot program was used to calculate areas from these silhouette images. After determining silhouette areas, all the needles were removed from each stem, and projected one-sided areas of all the needles were measured as described earlier. The ratio of silhouette to single-sided projected needle areas (SPAR) was calculated for each measurement period. Lower ratios indicate either greater self-shading and/or needle orientations that are not perpendicular to the solar beam.

Calculation of Daily Integrated Carbon Gain

To calculate daily carbon gain under ambient conditions, instantaneous rates of photosynthesis were integrated throughout each measurement day by calculating the areas under the curves between each measurement time, and subtracting respiration when found. Although gas exchange measurements started and ended at slightly different times at each of the elevations, carbon gain calculations reflect the same daily period of time among sites within each gas exchange campaign (June campaign: 3:58 – 18:34 solar time; July campaign: 4:50 – 13:06 solar time; October campaign: 7:18 – 16:16 solar time).

Fluorescence Measurements

Dark-adapted leaf chlorophyll fluorescence measurements were made in July 2015 on 3-5 branches on each of 3-5 trees at each gas exchange site using a Handy PEA Chlorophyll Fluorescence Meter (Hansatech Instruments Ltd., Norfolk, UK). Two to three needles on the south-facing side of the crown were inserted in the leaf clip and dark-adapted for a minimum of 30 min before measuring maximal efficiency of PSII (Fv/Fm). Measurement light intensity was 3,000 umol m^{-2} s^{-1} for 1 second and all measurements were made simultaneously or just after the gas exchange measurements.

C:N Ratios

Carbon and nitrogen contents were determined for Y2, Y1, and Y0 needles collected in August 2014. Needles were lyophilized using a Labconco FreeZone 6 at -70 °C and <0.1 mbar (Labconco, Kansas City, MO) for 7 days, then ground into a fine powder using a ball

mill (industrial paint can shaker) before being analyzed using a CNS elemental analyzer (FlashEA 1112 Series, Thermo Scientific Inc., Waltham, MA).

Needle Packing Density (NPD) and Specific Needle Mass (SNM)

There is the possibility that shoot- and needle-level architectural characteristics may adjust in response to elevational differences. To determine needle packing density, needles were removed and counted from 3-cm segments of Y0, Y1, and Y2 shoots from each of the 10 study trees at all 6 sites. Data were expressed as number of needles per linear cm of shoot.

Specific needle masses were calculated in order to examine needle-level adjustments to elevation differences. Needles used for gas exchange under ambient conditions and SPAR measurements were lyophilized and weighed with a Sartorius Practum 224 1S Analytical Balance (Sartorius AG, Göttingen, Germany) and specific needle mass was calculated as the ratio of dry needle mass to projected area (g/cm^2).

Statistical analyses

All statistical analyses were performed using Sigmaplot 13.0 and graphs were constructed using Microsoft Excel 2011 (Microsoft, Redmond, WA). Two-tailed *t*-tests were used to test for differences in light levels during the June gas exchange campaign, as well as peak photosynthetic rates of Y2 and Y1 needles in the June and July campaigns and of Y0 needles in the July and October campaigns. Site means were used in linear regression of final shoot lengths, total relative % increase in trunk diameter, and needle packing density (although trunk growth at high elevations was eliminated from regression, see text in Results section). One-way ANOVAs and post-hoc tests (Tukey's) were used to test for differences

among elevations in duration of bud expansion, shoot elongation, and trunk growth, as well as peak photosynthetic rates and light levels during the July and October campaigns, N and C content, and their ratios (using site means). Two-way ANOVAs and post-hoc tests (Tukey's) were used to test for the effects of elevation, needle age, and their interactions, on gas exchange rates under standard conditions, carbon gain during each of the diurnal campaigns and of all three diurnal campaigns combined, specific needle masses, and gas exchange and Fv/Fm during the 2015 campaign. Though many of these measurements were repeated throughout the season, RM-ANOVA was not appropriate because inferences were drawn among elevations and needle ages, not throughout time. If assumptions for parametric tests were not met, non-parametric alternatives were used. Significance for all analyses was assumed if $p < 0.05$.

Results

Microclimate

Daily maximum temperatures declined with increasing elevation, and essentially matched the moist adiabatic lapse rate of 7 °C increase per 1000 m reported by Bolstad et al. (1998) for the southern Appalachian Mountains. Daily maximum temperatures at middle elevation were 2.5 °C higher (expected: 1.4 °C) and at low elevation were 3.8 °C higher (expected: 3.6 °C) than at high elevation (Table 2). Daily mean temperatures also matched expectations, with middle elevation 0.3 °C higher (expected 1.0 °C) and low elevation 1.6 °C higher (expected 2.6 °C). However, daily minimum temperatures did not match expected trends (expected 3 °C increase per 1000 m decrease vs. 1.0 °C lower at middle elevation and 0.5 °C lower at low elevation), likely due to local topography and associated cold-air drainage at night and early in the mornings (see discussion section).

Daily maximum VPD was highest at low elevation (1.53 vs. 1.02 and 0.97 kPa at middle and high elevations, respectively), as was daily evaporative demand (11.21 vs. 7.02 and 9.54 $kPa*hd^{-1}$). However, minimum and average VPD and daily evaporative demand were lowest at middle elevation, again due to local topography and associated cold-air drainage and high humidity in the early morning at that site.

Daily average solar radiation decreased as elevation increased (202.4, 191.1, and 186.7 W/m^2) as did daily total insolation (4858, 4586, and 4465 $W*h\ m^{-2}\ d^{-1}$) at low, middle, and high elevations, respectively, likely due to a higher frequency of cloud events (either cloud-immersion or cloud-cover) at middle and high elevations. Average and maximum wind speeds were also highest at high elevation. Precipitation (from May 25 to October 31) was similar between low and high elevations (405 and 403 mm), but ~50 mm higher at middle

elevation (456 mm). This led to significantly higher soil moisture throughout the growing season at middle and high elevations (means: 27, 30, and 20 % at low, middle and high elevations, respectively; $p < 0.05$, Lauren Wood 2016, in preparation).

Table 2. Microclimatic conditions during the period May 25th – October 31st 2014. Each parameter was sampled every 2 seconds and averaged on 10-minute intervals. Parameter values, with the exception of cumulative precipitation, are means ± s.e. of all days ($n = 160$). All 10-minute intervals during a day were used to calculate mean daily air temperature, VPD, and wind speeds.

Parameters	Low Elevation	Middle Elevation	High Elevation
Mean daily air temperature (°C)	18.2 ± 0.4	16.9 ± 0.3	16.6 ± 0.3
Daily minimum air temperature (°C)	12.5 ± 0.4	12.0 ± 0.3	13.0 ± 0.3
Daily maximum air temperature (°C)	25.6 ± 0.4	23.1 ± 0.4	21.8 ± 0.4
Mean daily VPD (kPa)	0.47 ± 0.02	0.29 ± 0.01	0.40 ± 0.01
Daily minimum VPD (kPa)	0.03 ± 0.00	0.01 ± 0.00	0.17 ± 0.01
Daily maximum VPD (kPa)	1.53 ± 0.06	1.02 ± 0.04	0.97 ± 0.04
Daily evaporative demand (kPa*h/d)	11.21 ± 0.48	7.02 ± 0.33	9.54 ± 0.37
Mean daily solar radiation (W/m^2)	202.4 ± 6.7	191.1 ± 6.3	186.7 ± 6.4
Daily total insolation ($W*h\ m^{-2}\ d^{-1}$)	4858 ± 160	4586 ± 152	4465 ± 156
Mean daily wind speed (m/s)	0.43 ± 0.02	0.40 ± 0.02	0.98 ± 0.06
Daily maximum wind speed (m/s)	4.89 ± 0.12	4.39 ± 0.11	6.21 ± 0.22
Cumulative Precipitation (mm)	405	456	403

Phenology: Bud-burst

Release from dormancy and complete bud-burst occurred sooner at low than at either middle or high elevations. Buds at low elevation reached phenological stage 4 5 days sooner and stage 7 (complete bud-burst) 6 days sooner than at either middle or high elevations (Fig. 2). The duration of bud growth at low elevation (35 days) was 5 days shorter (Fig. 3, p = 0.0226) than at high elevation (40 days).

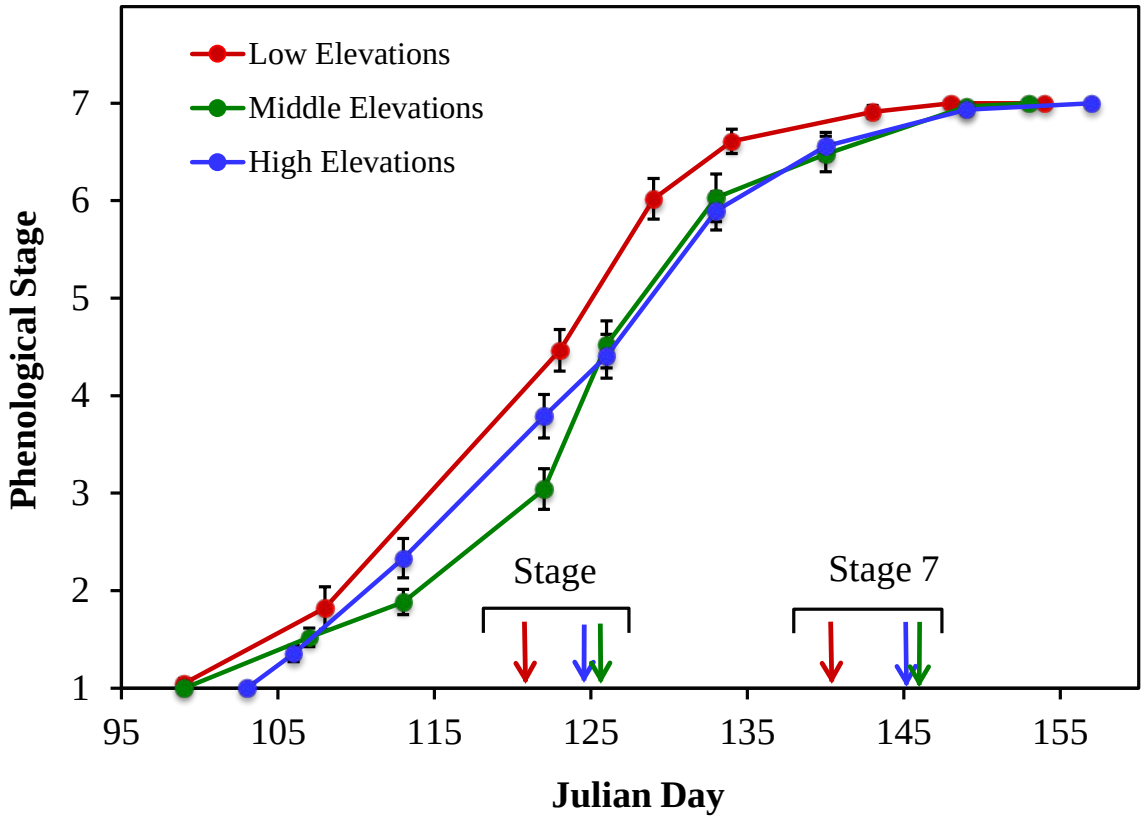

Figure 2. Seasonal timing of progression through phenological stages and bud-burst at each elevation. Phenological stage 1 represents dormant, waxy buds, and stage 7 indicates complete bud-burst. Phenological stage of 9 buds per tree was recorded weekly at all sites (540 buds total) and then averaged per tree. Points are mean phenological stage ± s.e. of 20 trees at each elevation. Arrows indicate dates that buds reached stage 4 and stage 7 at each elevation.

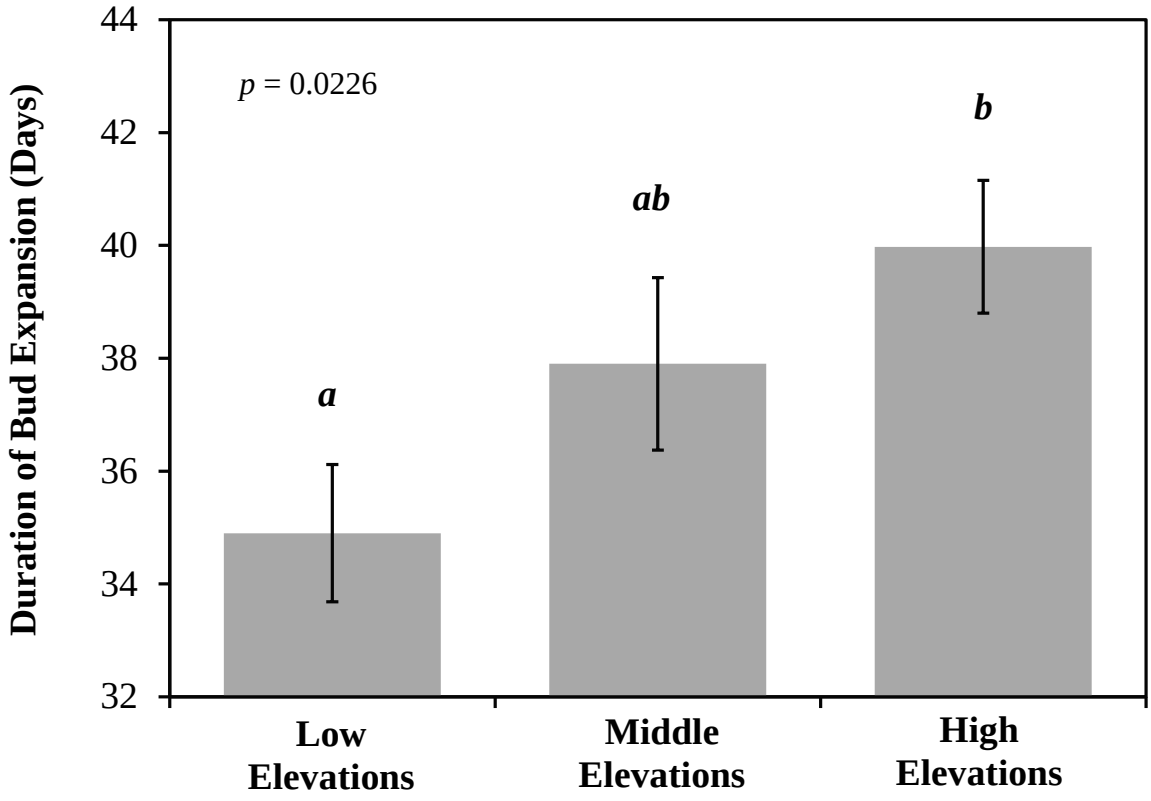

Figure 3. Duration of bud expansion after release from dormancy at each elevation. Bud expansion occurred during days 104-139, 103-141, and 105-145 at low, middle, and high elevations, respectively. Bars are means ± s.e. of 20 trees per elevation. Means that do not share the same letter indicate significant ($p < 0.05$) differences in duration of bud expansion among elevation categories.

Phenology: Shoot elongation

Elongation of new shoots began sooner at low than at either middle or high elevation sites. Shoots at low elevations reached 75% of their final lengths 8 days sooner than at middle and high elevations, and 95% of their final lengths 10 days sooner than at middle and high elevations, respectively (Fig. 4). Duration of shoot growth (days after bud-burst until shoots reached 95% of their final lengths) did not differ among elevations (Fig. 5, p =

0.0549). Final shoot lengths did not vary as a function of elevation (Fig. 6, r^2 = 0.02386, p = 0.7701). However, there was a significant difference in the final shoot length between the two higher-elevation sites (p = 0.015).

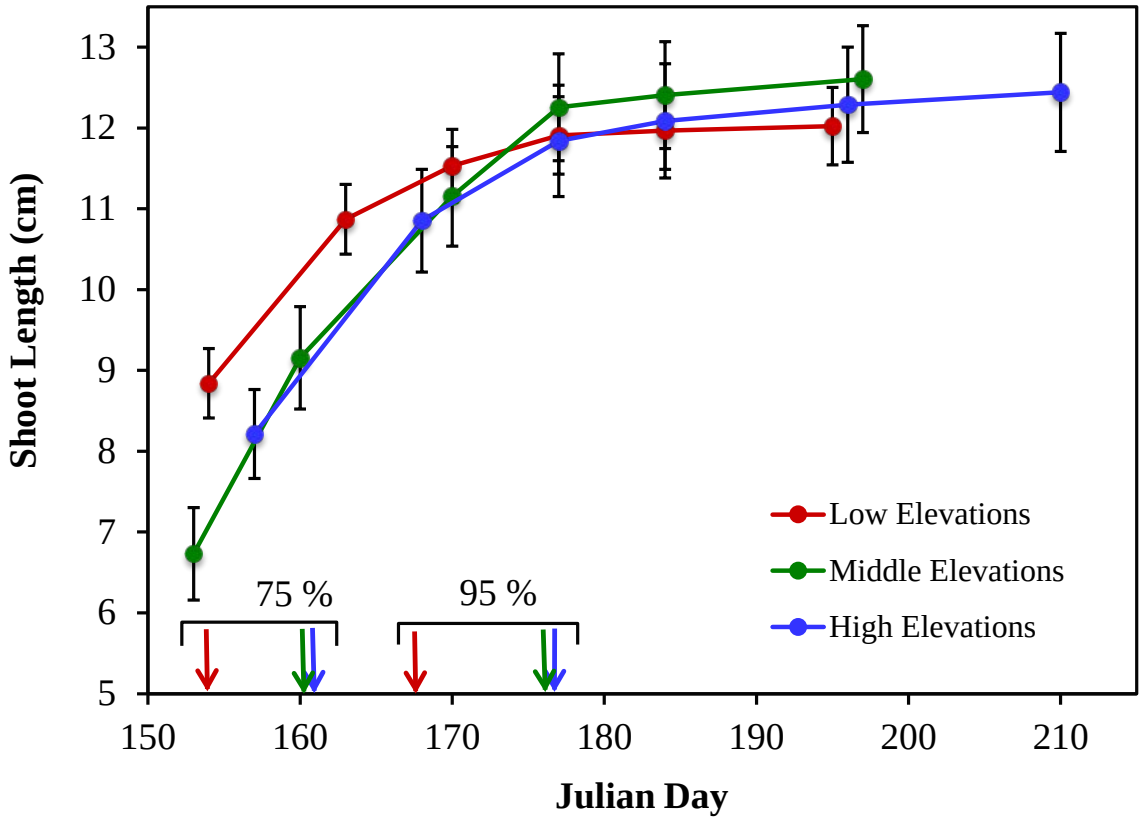

Figure 4. Seasonal timing of shoot elongation. After buds emerged, length of 9 shoots per tree was recorded weekly (540 shoots total) and then averaged per tree. Points are the mean shoot length ± s.e. of 20 trees per elevation. Arrows indicate dates that shoots reached 75 and 95% of their final lengths.

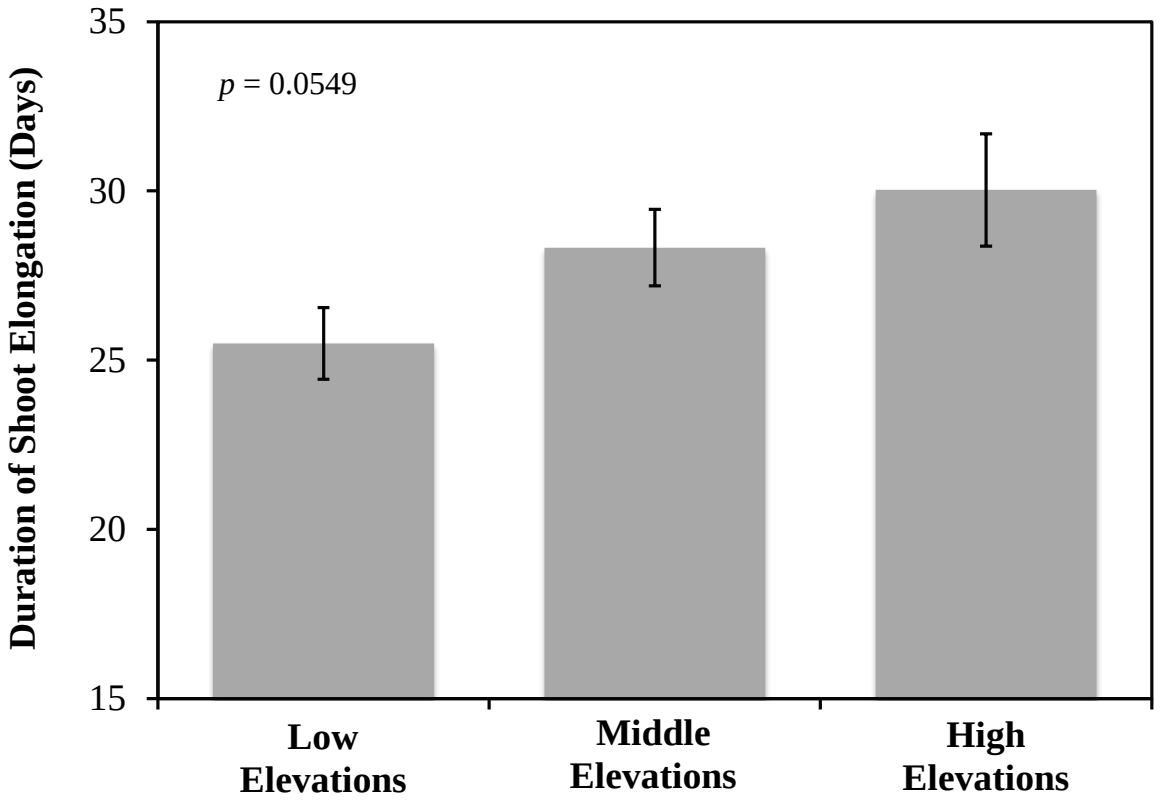

Figure 5. Duration of shoot elongation, spanning from the day that buds reached phenological stage 7 until 95% of their final lengths. After buds emerged, length of 9 shoots per tree was recorded weekly (540 shoots total) until elongation ceased and then averaged per tree. Shoot elongation occurred during days 139-164, 141-169, and 145-175 at low, middle, and high elevations, respectively. Bars are means ± s.e. of 20 trees per elevation.

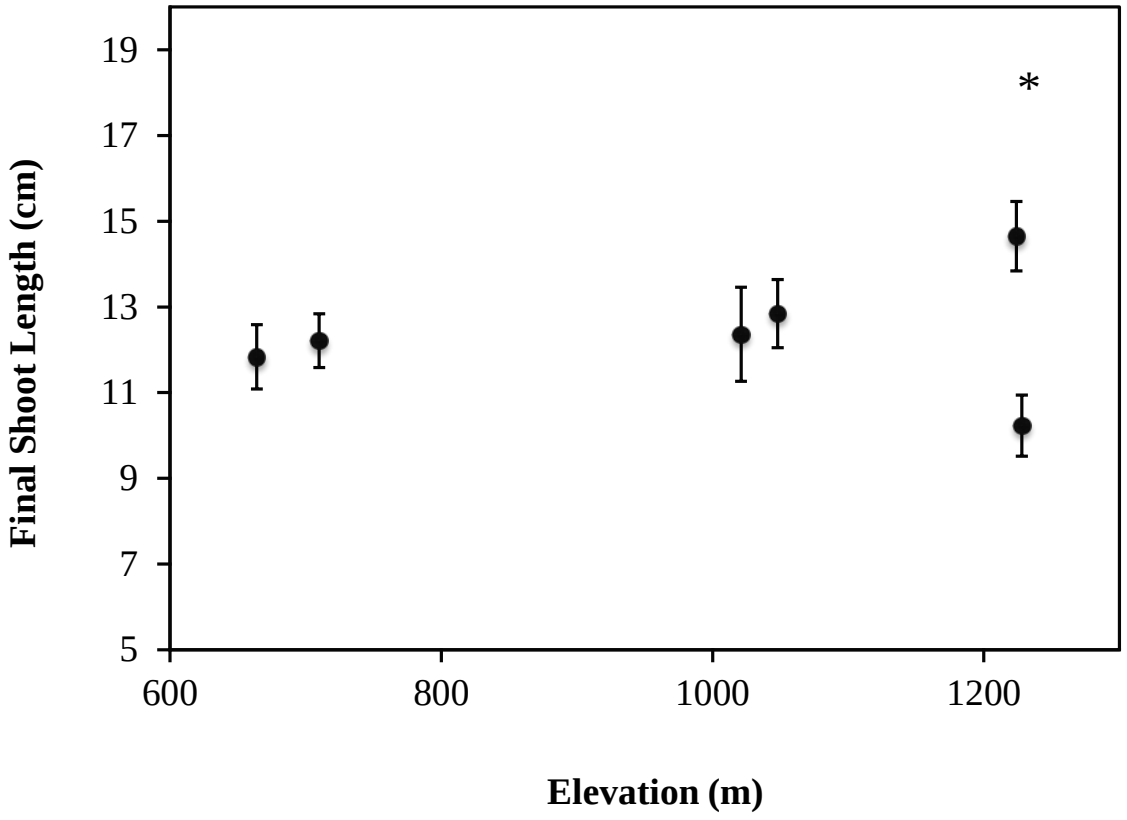

Figure 6. Final shoot lengths as a function of elevation. After shoot elongation ceased, lengths of 9 shoots per tree were averaged. Points are mean length ± s.e. of 10 trees per site. Asterisk denotes a significant difference (p = 0.015) between the two sites at high elevation.

Phenology: Trunk growth

Both the timing and magnitude of trunk diameter growth varied among elevations. Trunk growth was delayed at low elevations, with trunks reaching 50% of their total % increase in diameter 10 and 18 days later, and 95% 3 and 8 days later, than at middle and high elevations respectively (Fig. 7). Duration of trunk growth was 9 days shorter (115 days, $p = 0.014$) at high elevation than at middle and low elevations (mean: 124 days), which did not differ from each other (Fig. 8).

Percent increase in trunk diameter throughout the season was highest at the middle elevation (Fig. 9), although there was appreciable variation between the two sites at high elevation. A nested ANOVA (trees nested within site, and two sites nested within elevation category) was used to test for contributions of variation among and within elevation categories. This analysis showed that elevation explained the majority of the total variation (83%, $p < 0.0001$), and post-hoc tests revealed that total trunk growth was equal between the two low- and two middle-elevation sites, but differed between the two high-elevation sites, just as did shoot length. When the two sites at high elevation were eliminated, differences in total trunk growth between low and middle elevations became highly significant (Fig. 9, $r^2 = 0.9754$, $p = 0.0124$).

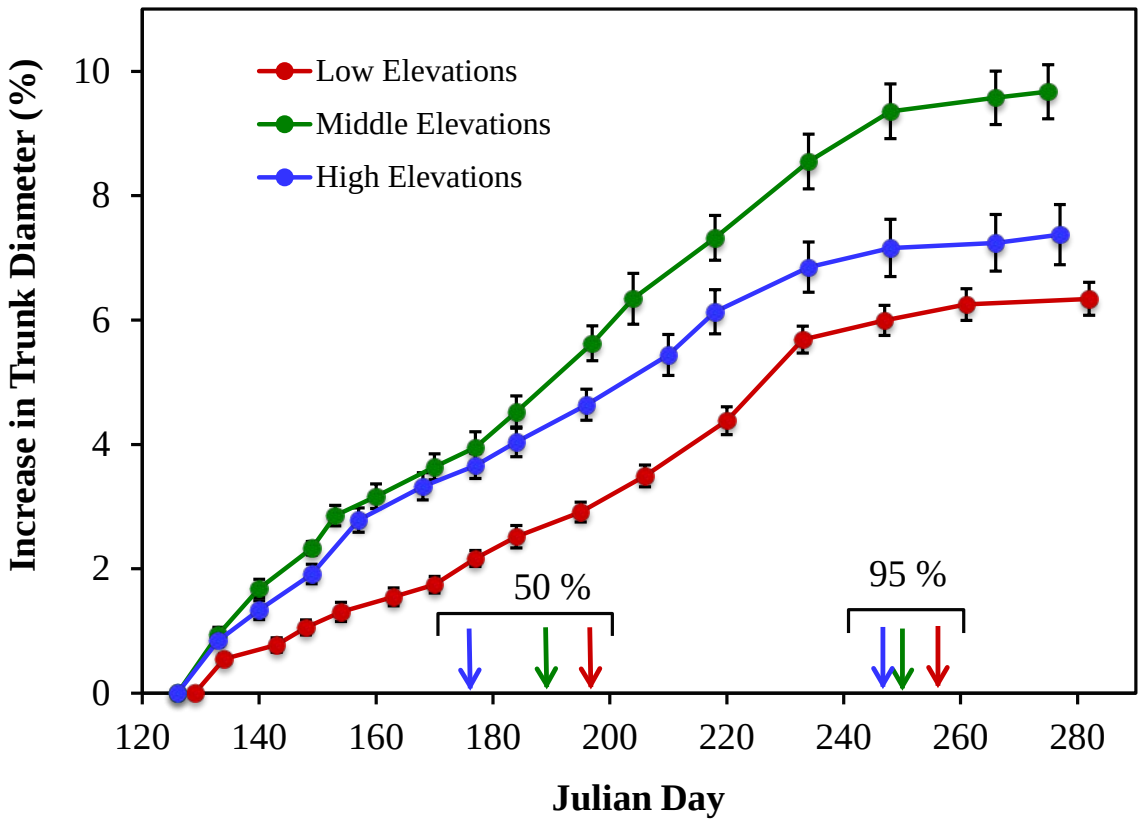

Figure 7. Seasonal timing and magnitude of trunk growth at each elevation. Growth of each tree was expressed as % increase compared to its diameter at the beginning of the season, and points are means ± s.e. of 20 trees per elevation. Arrows indicate dates when trunks reached 50 and 95 % of their total increase in diameter throughout the season.

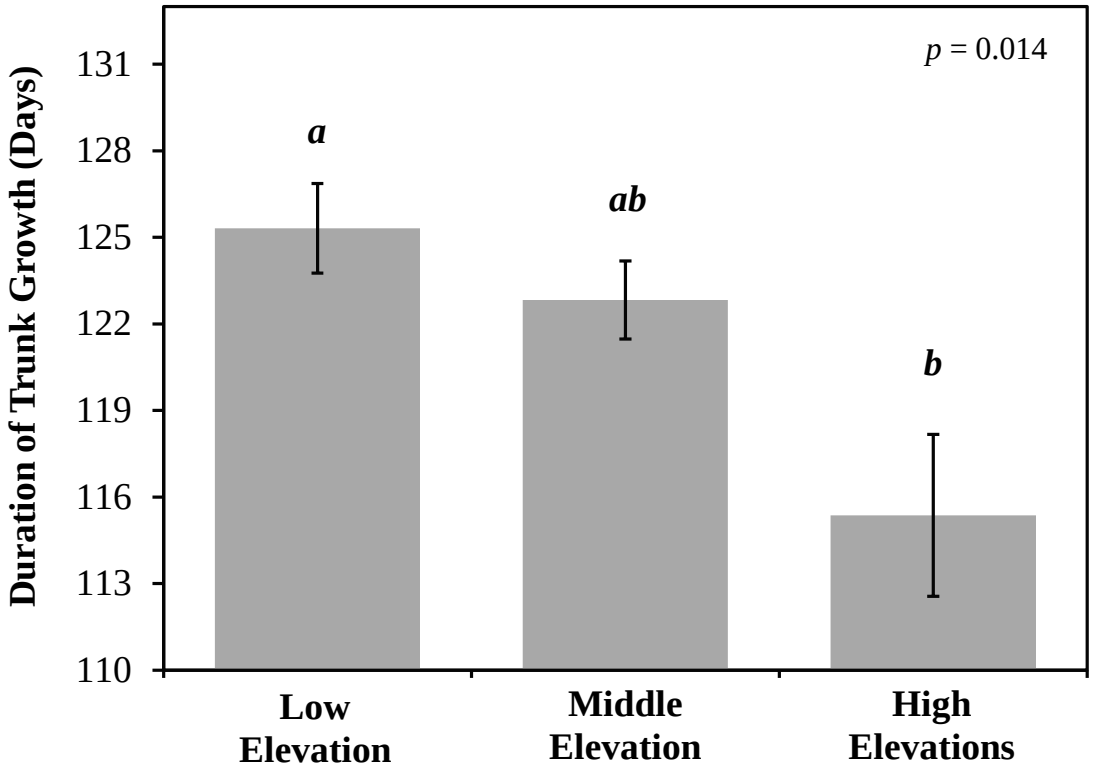

Figure 8. Duration of trunk growth at each elevation. Growth of each tree was expressed as % increase compared to its diameter at the beginning of the season, and duration of growth spans from the beginning of trunk growth until each tree reached 95% of its total growth at the end of the season. Trunk growth occurred during days 130-255, 130-252, and 132-247 at low, middle, and high elevations, respectively. Bars are means ± s.e. of 20 trees per elevation. Means that do not share the same letter indicate significant ($p < 0.05$) differences in duration of trunk growth among elevations.

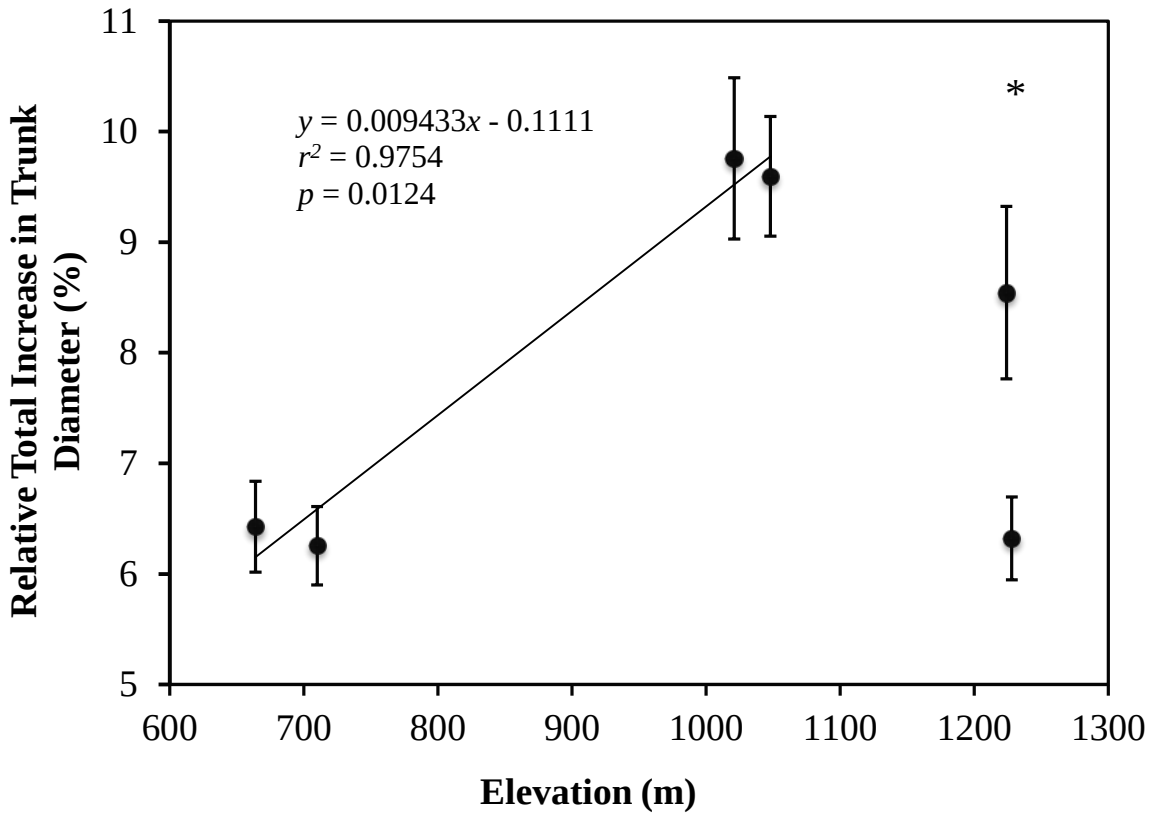

Figure 9. Relative total % increase in trunk diameter as a function of elevation. Points are means ± s.e. of 10 trees per site. Asterisk indicates significant difference ($p < 0.05$) in trunk growth between the two sites at high elevation. When these two sites were eliminated, a linear regression for low and middle elevations sites was highly significant.

Gas Exchange under Standard Conditions

Neither A_{net} (Fig. 10a) nor R_d (Fig. 10b) varied among elevations (A_{net}: $p = 0.567$, R_d: $p = 0.399$) under standard conditions, and both parameters decreased as needles aged (A_{net}: $p < 0.001$, R_d: $p = 0.028$). Photosynthetic rates of 1-year-old (Y1) and 2-year-old (Y2) needles were only 82% and 48% of the rates of current year needles (Y0), respectively. Similar trends were found for R_d (Y1 and Y2 were 73% and 43% of Y0, respectively).

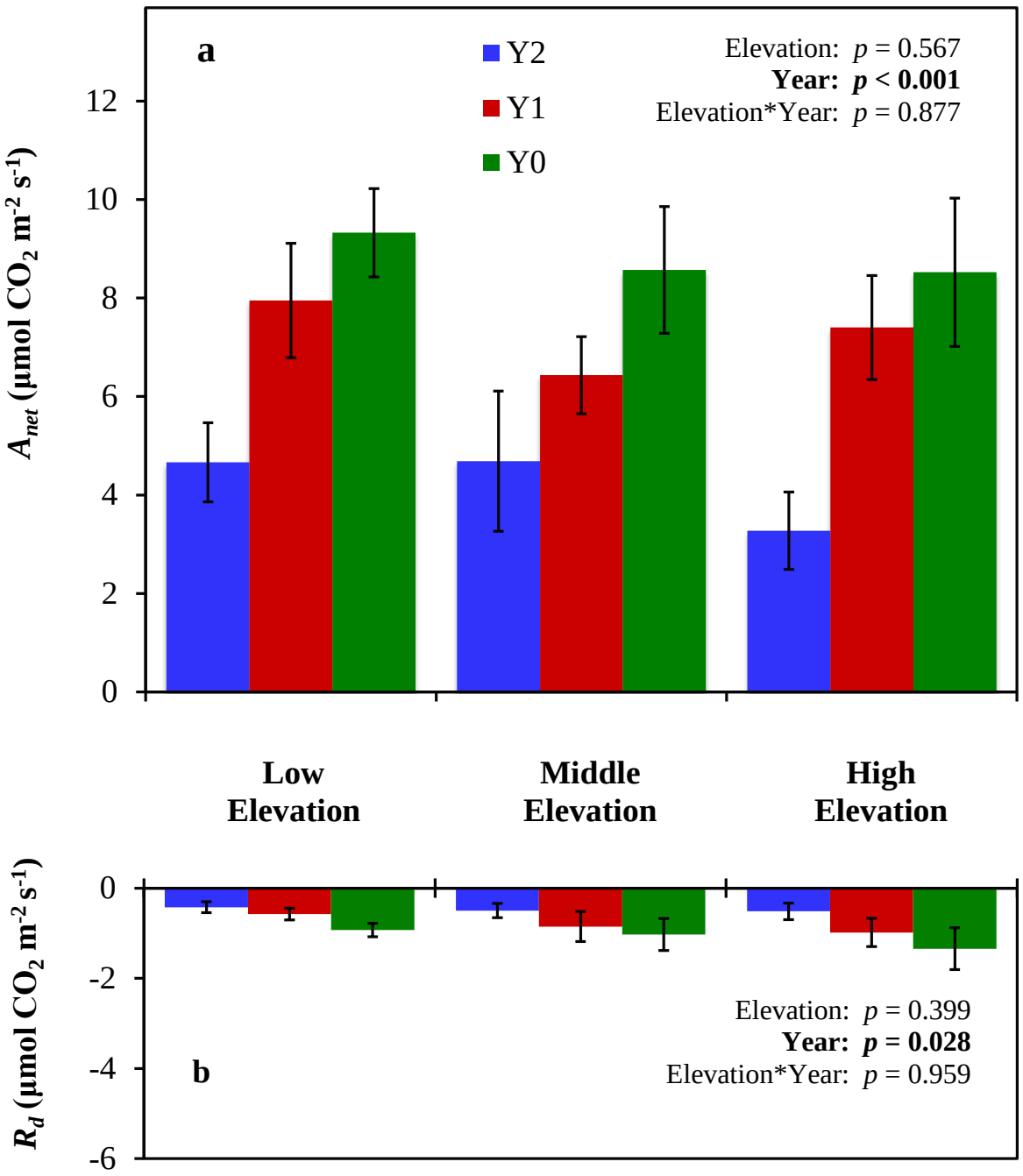

Figure 10. Photosynthesis (a) and dark respiration (b) of Y2, Y1, and Y0 needles under standard conditions (see text). Points are means ± s.e of 5 trees per elevation.

Nitrogen and Carbon Content

Needle nitrogen and carbon contents (%), and their ratio, were determined for Y1 needles collected in August 2014 from 5 trees per site, and site means were used in ANOVAs (n = 2 sites per elevation category). Nitrogen content ranged from 1.15 to 1.71% (site means) and was significantly lower at high elevation than at middle and low elevations, which did not differ from each other (Fig. 11, p = 0.0476). Carbon content did not vary among elevation categories (Fig. 12, p = 0.4564), nor did the ratio of carbon to nitrogen (Fig. 13, p = 0.0879).

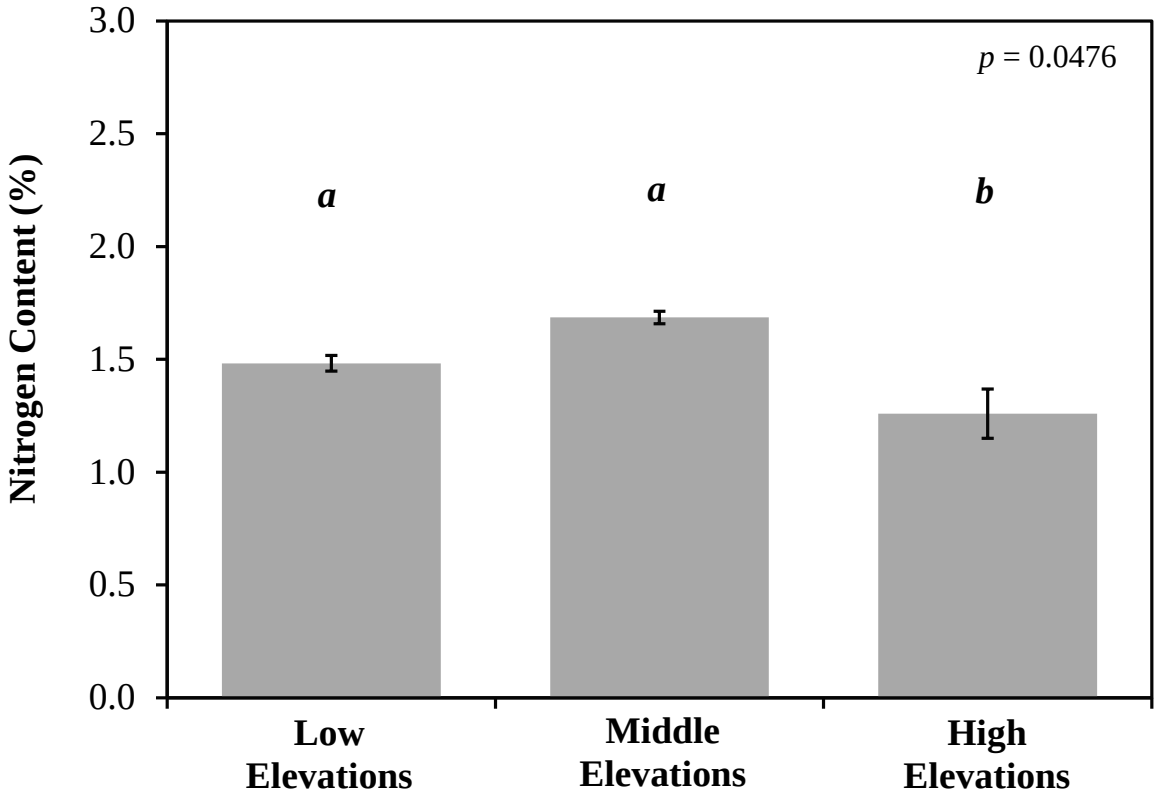

Figure 11. Nitrogen content of needles collected in August 2014. Mean nitrogen contents of one year old needles (Y1) from 5 trees were determined for each site. Bars are means ± s.e. of 2 sites per elevation category. Bars that do not share the same letter indicate significant differences in nitrogen content among elevation categories.

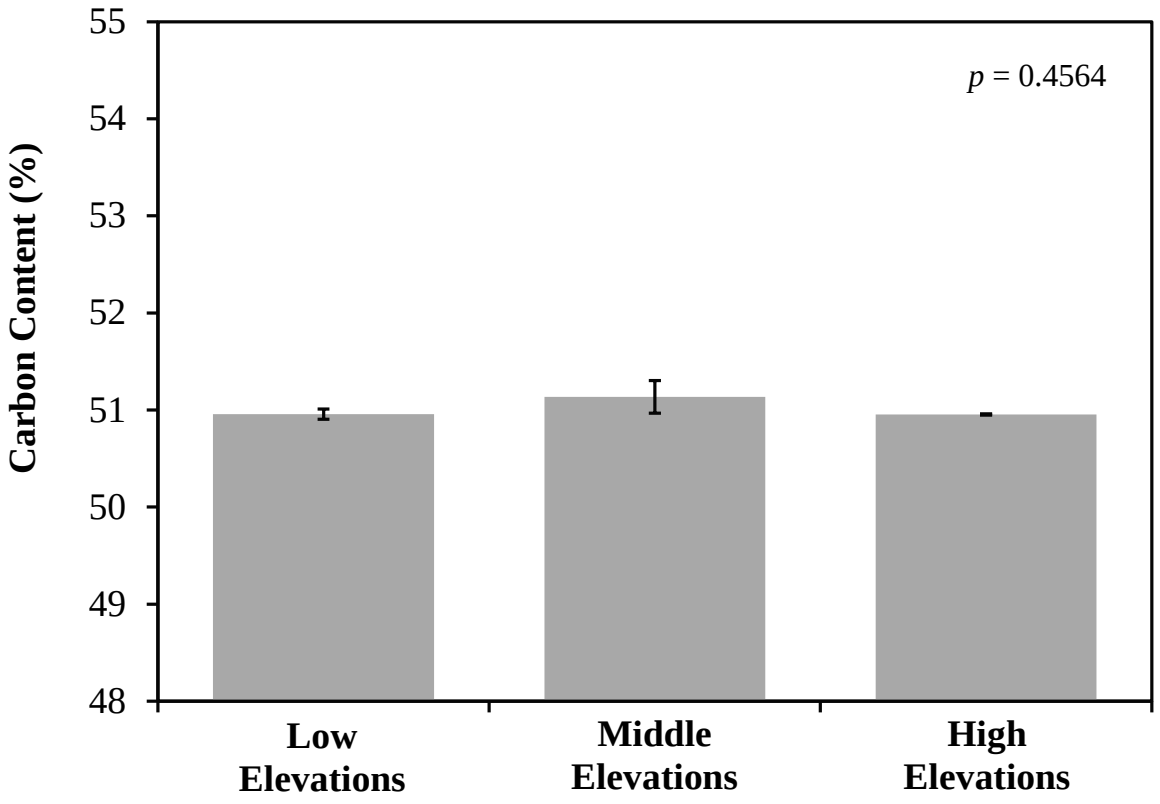

Figure 12. Carbon content of needles collected in August 2014. Mean carbon contents of one year old needles (Y1) from 5 trees were determined for each site. Bars are means ± s.e. of 2 sites per elevation category.

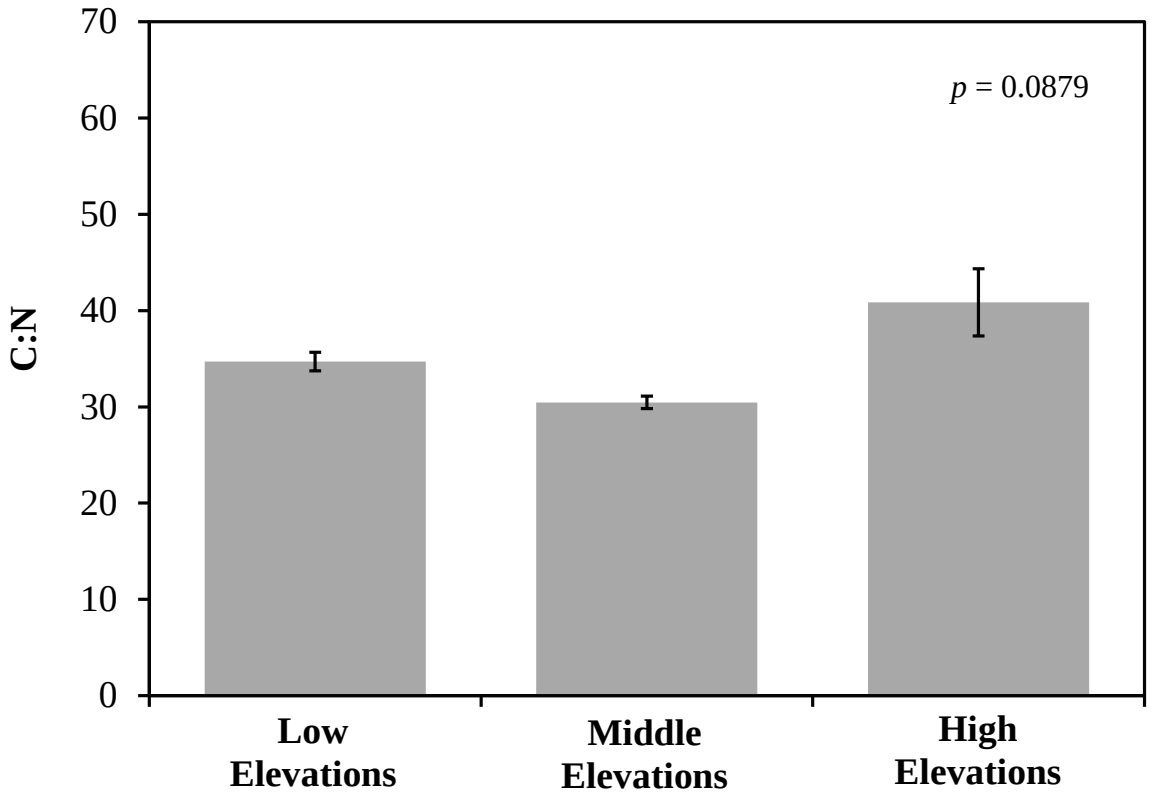

Figure 13. Ratio of carbon content to nitrogen content needles collected in August 2014. Mean C:N of one year old needles (Y1) of 5 trees were determined for each site. Bars are means ± s.e. of 2 sites per elevation category.

Gas exchange under ambient conditions

June 2014 Measurements

Due to the logistical constraints of conducting diurnal gas exchange measurements across the elevational gradient, each site was sampled on a separate day (see Table 3 for dates). During these measurements, maximum temperatures were 32.8, 24.0, and 23.1 °C at low, middle, and high elevation sites respectively (Table 3). The low elevation site was significantly hotter than would be expected due to the adiabatic lapse (mean and maximum

temperatures 5.6 and 9.7 °C hotter than high elevation; expected only 2.6 and 3.6 °C hotter). In fact, the highest seasonal maximum temperatures occurred at the low elevation site during this measurement period. As a result, the maximum leaf-to-air vapor pressure deficit and daily evaporative demand at this site (3.04 kPa, 22.14 kPa*h) were the highest of any day throughout the entire season, and much higher than during measurement days at either the middle or high elevation sites (1.26 and 0.83 kPa, 9.55 and 8.23 kPa*h). Cloud events occurred more often throughout the day and during measurement periods at high elevation, occasionally reducing solar radiation to <15 % of full sunlight (Fig. 14f, 0.167 kW/m^2 at 12:20 solar time, full sunlight: 1.14 kW/m^2), resulting in lower integrated insolation (4.99 $kW*h/m^{-2}$) than at the low and middle elevation sites (7.98 and 7.74 $kW*h/m^2$).

Photosynthesis of all trees at low elevation reached its daily maximum early in the morning (6:50 solar time), but peaked at mid-day (13:05 solar time) at middle elevation, and even later in the afternoon (15:50 solar time) at high elevation (Fig. 14a-c). Peak photosynthetic fluxes of Y1 needles at high and middle elevations were 107% and 141% higher ($p = 0.0207$) than at low elevation; elevational trends of Y2 needles were not significant ($p = 0.1476$).

Rates of photosynthesis declined as needles aged. Peak photosynthetic rates of Y2 needles were only 42% of the rates of Y1 needles ($p = 0.0008$). Although gas exchange measurements under standard conditions demonstrated that intrinsic photosynthetic capacity is reduced in older needles (Fig. 10a), the effect of age on photosynthetic rates under ambient conditions is also driven by differences in light environment within the canopy. Current-year shoots receive more direct sunlight because of their location on the exterior of the canopy while older shoots are located deeper within the canopy and receive less direct light and

probably relatively more diffuse sunlight. PAR during these gas exchange measurements peaked at 756 ± 157 μmol m^{-2} s^{-1} for Y1 shoots, but only 136 ± 62 μmol m^{-2} s^{-1} for Y2 shoots (means ± s.e., $p = 0.001$).

Daily carbon gain (calculated during the period 3:55 - 18:34 solar time at all sites) varied depending on elevation and needle age (Fig. 15). Daily carbon gain was nearly halved at low elevation compared to the other two elevations, which did not differ from each other ($p < 0.001$). As with instantaneous rates, daily carbon gain was significantly lower in older (Y2) needles, with Y1 needles accounting for 71 % of total carbon gain ($p < 0.001$), and this partitioning was consistent across all three elevations.

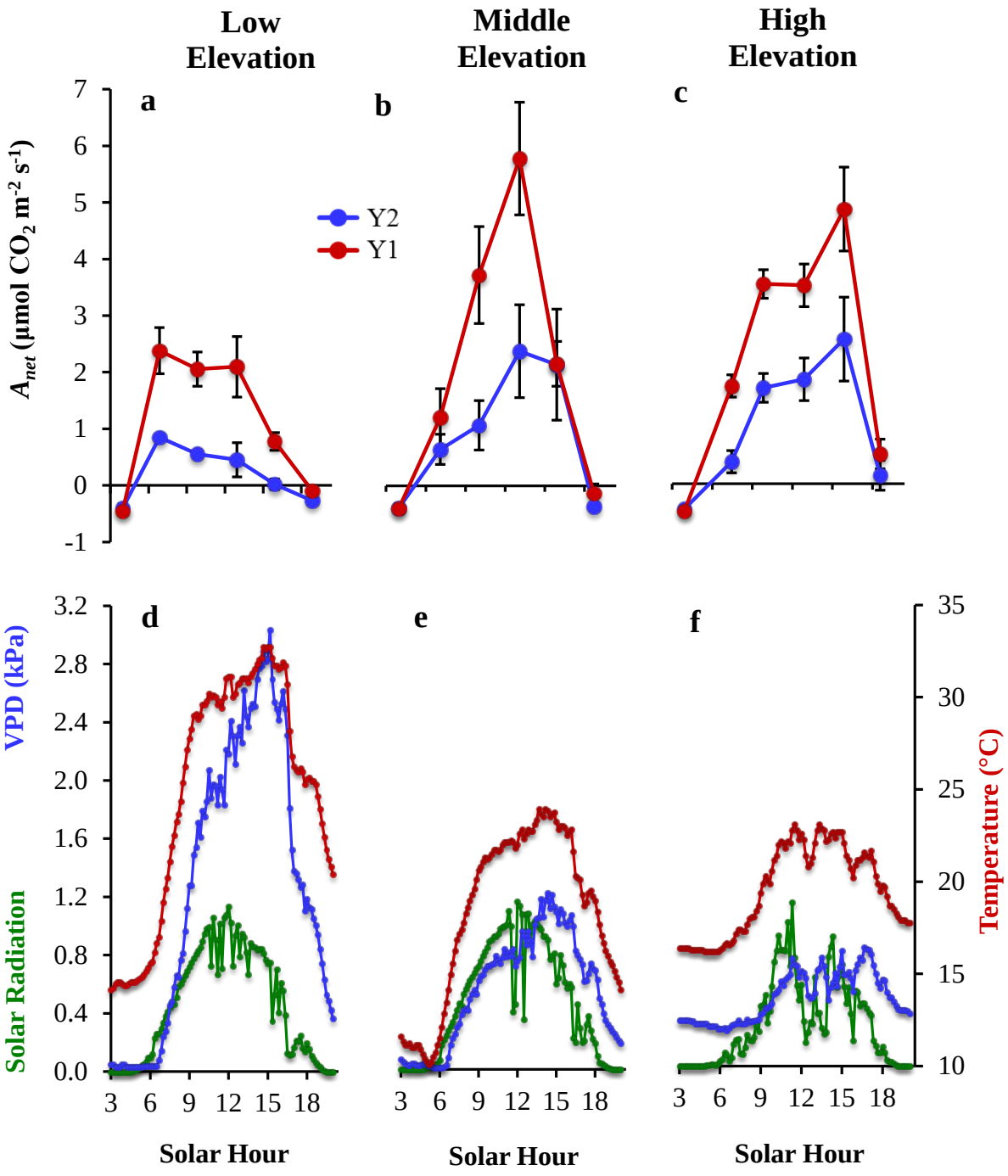

Figure 14. (a-c) Diurnal patterns of photosynthesis of Y2 and Y1 needles, and (d-f) solar radiation (green lines, left axis), VPD (blue lines, left axis), and temperature (red lines, right axis) during in June 2014. Points in a-c are means ± s.e. of 5 trees. Microclimate parameters are means of 10-min intervals sampled every 2 seconds.

Table 3. Microclimate parameters during each day of diurnal gas exchange measurements under ambient conditions in June 2014. Parameters were sampled every 2 seconds and averaged on 10-minute intervals from 3:00-20:00 solar time. Mean air temperatures and VPD are means ± s.e. of all 10-minute intervals.

	Low Elevation	Middle Elevation	High Elevation
Measurement Date	June 18	June 2	June 8
Mean Air Temperature (°C)	25.1 ± 0.6	18.4 ± 0.4	19.5 ± 0.2
Minimum Air Temperature (°C)	14.4	10.3	16.2
Maximum Temperature (°C)	32.8	24.0	23.1
Mean VPD (kPa)	1.29 ± 0.10	0.56 ± 0.04	0.48 ± 0.02
Minimum VPD (kPa)	0.03	0.01	0.25
Maximum VPD (kPa)	3.04	1.22	0.83
Evaporative Demand (kPa*h)	22.14	9.55	8.23
Total Insolation ($kW*h/m^{-2}$)	7.74	7.98	4.99

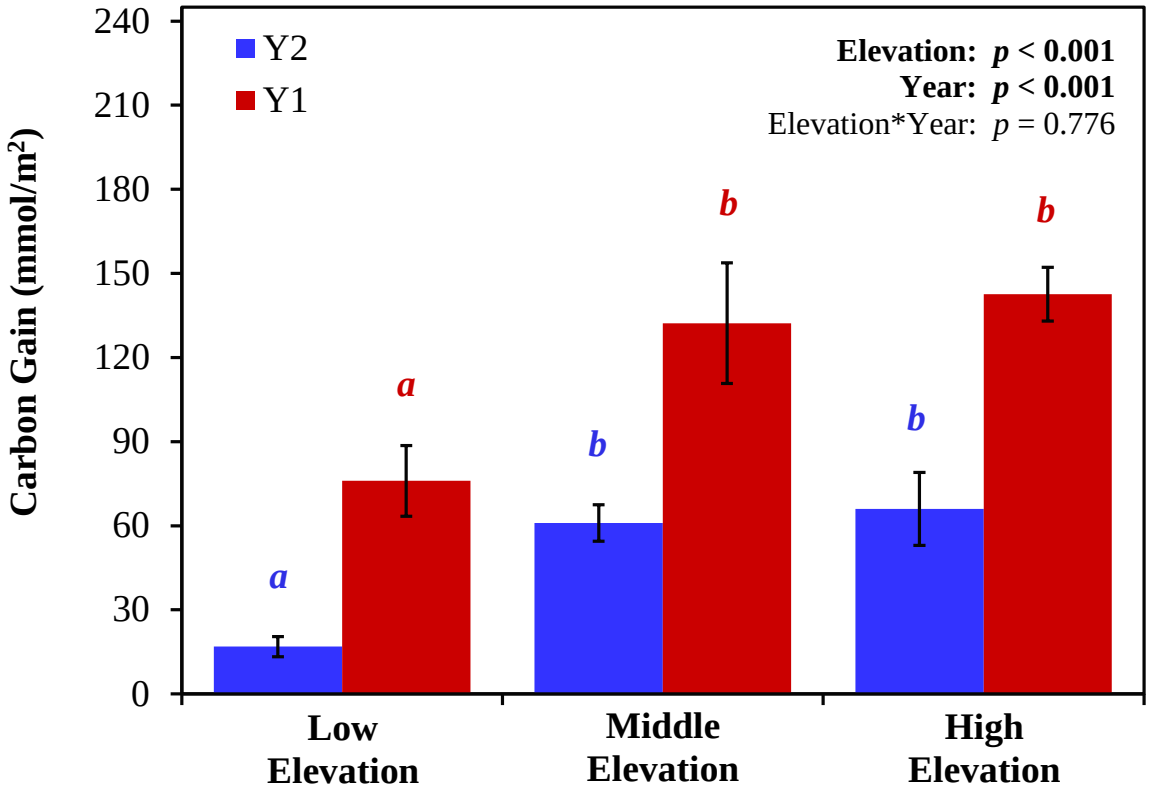

Figure 15. Daily carbon gain of Y2 and Y1 needles in June 2014. Bars are means ± s.e. of 5 trees per elevation. Letters indicate significant differences ($p < 0.05$) in daily carbon gain among elevations within a needle cohort (red = 1 year old needles, blue = 2 year old needles).

July 2014 Measurements

During gas exchange measurements in July 2014 (see Table 4 for dates), mean temperatures from 3:00 – 20:00 solar time were 22.3, 21.0, and 15.7 °C, and maximum temperatures were 27.8, 27.2, and 19.4 °C, at low, middle, and high elevation sites respectively (Table 4). The high elevation site was significantly colder than the middle and low elevation sites, much more so than would be expected due to the adiabatic lapse rate; mean temperatures were 5.3 and 6.6 °C colder than at middle and low elevation sites (expected only 1.0 and 2.6 °C), and maximum temperatures were 7.8 and 8.4 °C colder

(expected only 1.4 and 3.6 °C). Maximum VPD was 1.48, 1.12, and 1.01 kPa at low, middle and high elevation sites respectively, but mean VPD and integrated evaporative demand were lowest at the middle elevation site (0.71, 0.34, and 0.51 kPa; 12.25, 5.90, 8.79 kPa*h). This is because VPD remained very low (<0.03 kPa, occasionally 0.00) until 8:00 solar time at middle elevation, but remained >0.03 and >0.1 kPa during the same period at low and high elevations respectively (Fig. 16d-f). Cloud events did not occur at low elevation until ~13:00 solar time, but were frequent throughout the day and during measurement periods at middle and high elevations, occasionally reducing solar radiation to < 30 % of full sunlight (middle elevation: 0.194 kW/m^2 at 12:20 solar time; high elevation: 0.301 kW/m^2 at 11:50 solar time; full sunlight ≥ 1.05 kW/m^2 during 11:50 – 12:20 solar time).

Gas exchange measurements at the middle elevation site had to end at ~14:00 solar time (15:30 local time) due to a sudden afternoon thunderstorm. It had been relatively clear through early morning up to mid-day though. Photosynthesis of all trees at low and middle elevations reached a daily maximum before solar noon (Fig. 16a-b, 10:12 and 10:39 solar time), but peaked after solar noon at high elevation (Fig.16c, 13:06 solar time). Peak photosynthetic rates of Y0 needles did not vary among elevations (averaged 6.60 – 7.27 μmol CO_2 m^{-2} s^{-1}, $p = 0.8358$) and trends were consistent for other age needles (Y1: $p = 0.9905$, Y2: $p = 0.1287$). Seasonal differences were not significant; although Y0 needles were not included in June measurements, peak rates of older needles (Y1 and Y2) did not change between June and July (Y1: $p = 0.7632$, Y2: $p = 0.5788$).

As before, rates of photosynthesis were lower in older needles. Peak photosynthetic rates of Y1 needles were only 65% of Y0 needles, and Y2 needles were only 30%. The reduction in photosynthesis of older needles was driven in part by lower light levels deeper

within the canopy. PAR during gas exchange measurements peaked at 922 ± 181 μmol m^{-2} s^{-1} photons for Y0 shoots, but were only 437 ± 124 and 188 ± 90 μmol m^{-2} s^{-1} for Y1 and Y2 shoots (means ± s.e., $p = 0.0020$).

Daily carbon gain (calculated from 4:50 to 13:14 solar time at all sites) decreased as needles aged ($p < 0.001$), but did not vary among elevations (Fig. 17, $p = 0.307$). Carbon gain of these older Y1 and Y2 needles accounted for only 30% and 16% of total carbon gain respectively.

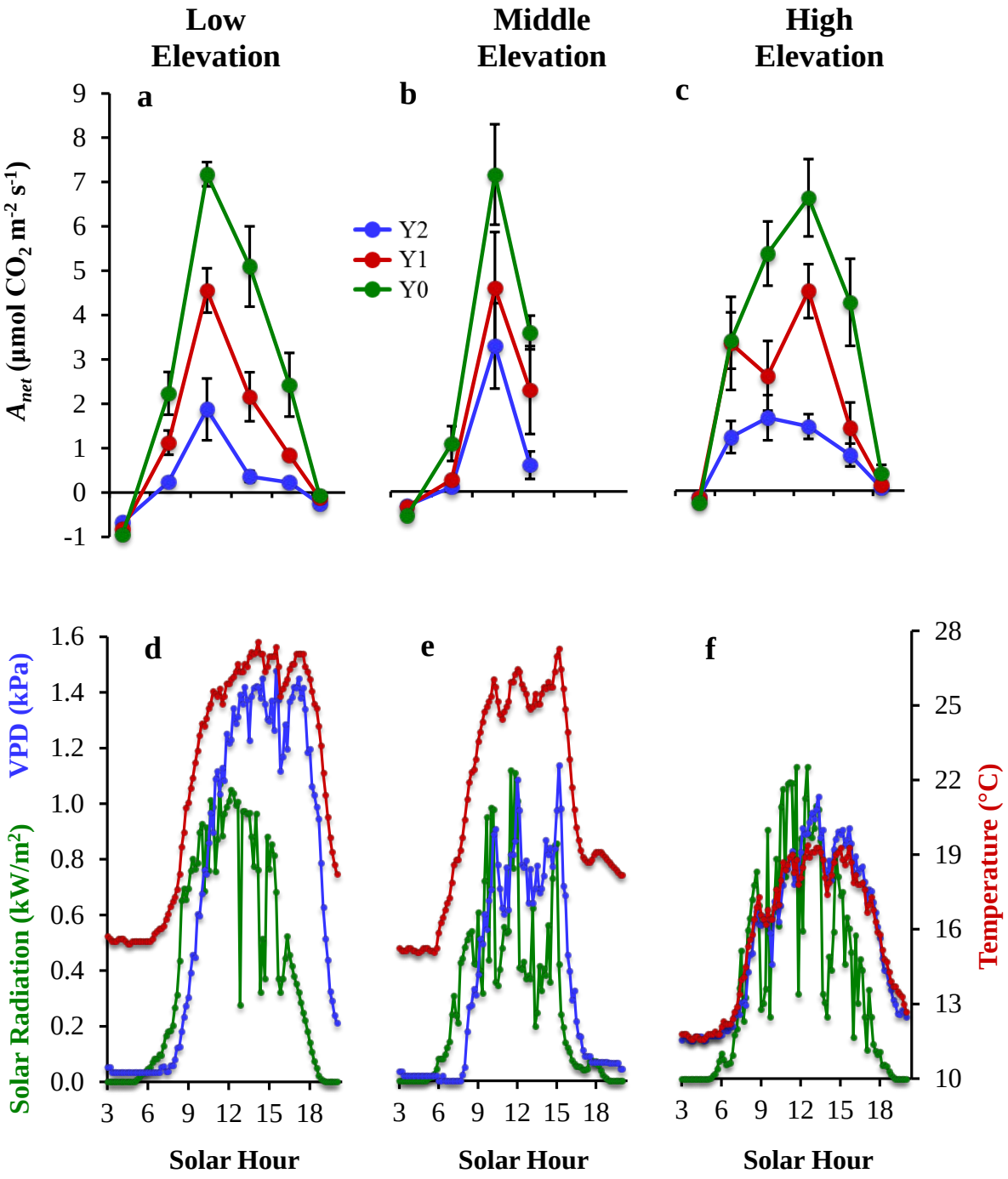

Figure16. (a-c) Diurnal patterns of photosynthesis of Y2, Y1, and Y0 needles, and (d-f) solar radiation (green lines, left axis), VPD (blue lines, left axis), and temperature (red lines, right axis) during in July 2014. Points in a-c are means ± s.e. of 5 trees per elevation. Microclimate parameters are means of 10-min intervals sampled every 2 seconds.

Table 4. Microclimate parameters during each day of diurnal gas exchange measurements under ambient conditions in July 2014. Parameters were sampled every 2 seconds and averaged on 10-minute intervals from 3:00-20:00 solar time. Mean air temperatures and VPD are means ± s.e. of all 10-minute intervals.

	Low Elevation	Middle Elevation	High Elevation
Measurement Date	July 25	July 23	July 29
Mean Air Temperature (°C)	22.3 ± 0.5	21.0 ± 0.4	15.7 ± 0.3
Minimum Air Temperature (°C)	15.6	15.1	11.6
Maximum Temperature (°C)	27.8	27.2	19.4
Mean VPD (kPa)	0.71 ± 0.06	0.34 ± 0.03	0.51 ± 0.03
Minimum VPD (kPa)	0.04	0.00	0.14
Maximum VPD (kPa)	1.48	1.12	1.01
Evaporative Demand (kPa*h)	12.25	5.90	8.79
Total Insolation ($kW*h/m^{-2}$)	7.21	4.65	6.26

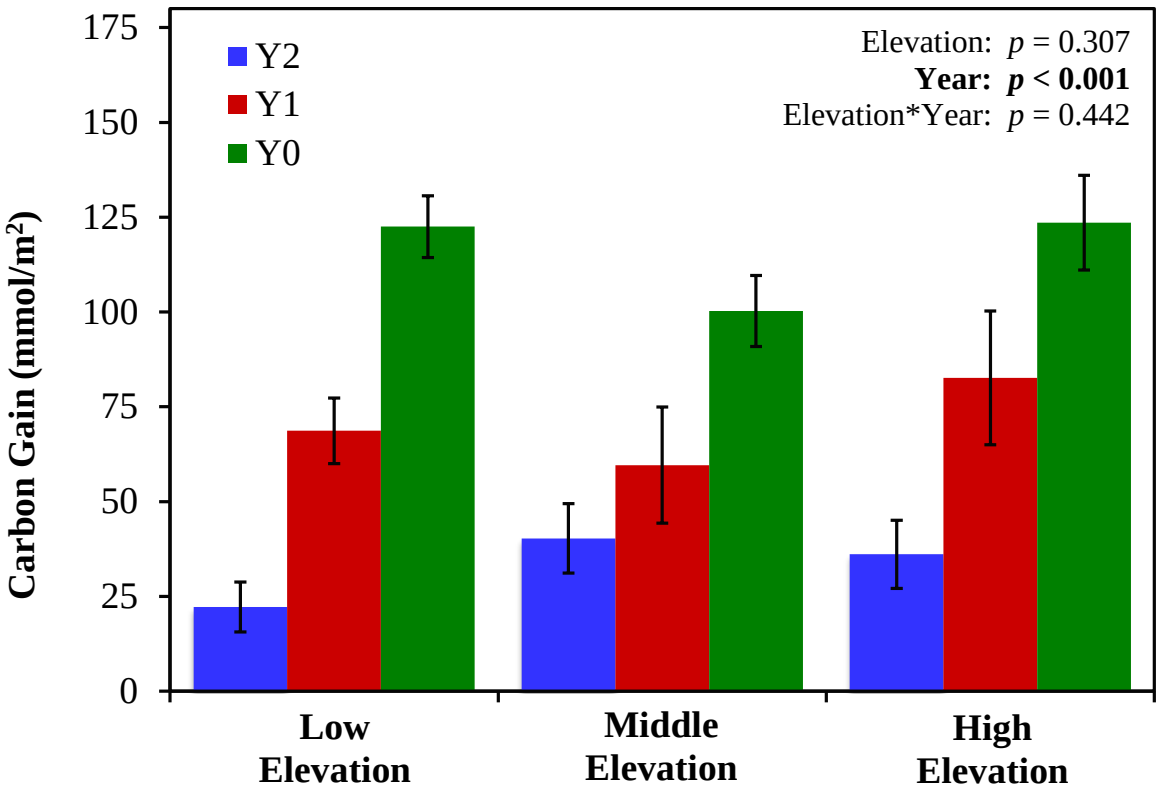

Figure 17. Daily carbon gain of Y2 (blue bar), Y1 (red bars), and Y0 (green bars) needles in July 2014. Bars are means ± s.e. of 5 trees per elevation.

October 2014 Measurements

Gas exchange measurements in October 2014 took place over two separate days at low elevation (see Table 5 for dates). On the first day (solid line in Fig. 18a), measurements had to end at ~13:40 solar time due to an afternoon thunderstorm. Therefore, additional measurements were made on a second day in October, beginning at 13:15 solar time, and continuing until dusk (dotted line in Fig. 18a). For carbon gain calculations (Fig. 19) and microclimate trends (Fig. 18d, Table 5), measurements at 13:40 on the first day were substituted by those at 13:15 on the second day. Weather data were incomplete after 11:00 solar time (12:30 local time) at middle elevation (Fig. 18e) due to technical failure of the

weather station. Although data from the weather station at middle elevation were incomplete, afternoon air temperatures during LI-Cor measurements were 5 °C hotter at middle elevation than at low elevation, and 17 °C higher than at high elevation. Mean temperatures from 3:00 – 20:00 solar time (measured by weather stations) were 13.2 and 4.8 °C, and maximum temperatures were 24.8 and 8.4 °C, at low and high elevation sites respectively. At all three elevations, early morning (3:00 solar time) temperatures ranged from 5-10 °C, and VPDs were <0.1 kPa (Fig. 18d-f). After sunrise (6:00 solar time), temperatures and VPDs increased at low and middle elevations but the arrival of a cold-front at the high elevation site reduced temperatures to 2.6 °C by 8:30 solar time. This cold front caused the high elevation site to be significantly colder than the low elevation site throughout the rest of the day, much more so than would be expected due to the adiabatic lapse rate; mean and maximum temperatures at high elevation were 8.4 and 16.4 °C colder than low elevation (expected only 2.6 and 3.6 °C colder). Although these two sites received similar integrated insolation (Table 5, 4.14 and 4.51 $kW*h/m^2$), mean and maximum VPD and integrated evaporative demand at high elevation were less than half of low elevation.

Peak photosynthetic rates of each of the three needle ages did not vary among elevations (Fig. 18a-c, Y0: $p = 0.4036$, Y1: $p = 0.4588$, Y2: $p = 0.0931$). Seasonal differences were not significant; rates of Y0 needles did not change between July and October ($p = 0.9909$), and rates of older needles were equivalent in June, July, and October (Y1: $p = 0.8589$; Y2: $p = 0.4044$).

As before, photosynthesis was lower in older needles, with rates of Y1 needles only 67% of Y0 needles, and Y2 needles only 36%. During these measurements, PAR peaked at

963 ± 99 μmol m^{-2} s^{-1} for Y0 shoots, but were only 431 ± 129 and 146 ± 57 μmol m^{-2} s^{-1} for Y1 and Y2 shoots (means ± s.e., $p < 0.0001$).

Daily carbon gain (calculated during the period 7:18 - 16:16 solar time at all sites) varied among needle ages and elevations, although their interaction was not significant (Fig. 19). Compared to low elevation, daily carbon gain of all ages combined was 20% lower at middle elevation, but 18% higher at high elevation (Fig. 19, $p < 0.001$). As before, carbon gain decreased as needles aged; Y1 and Y2 needles accounted for only 31 and 16% of total carbon gain in October, and the relative contributions of each needle age were the same as July measurements.

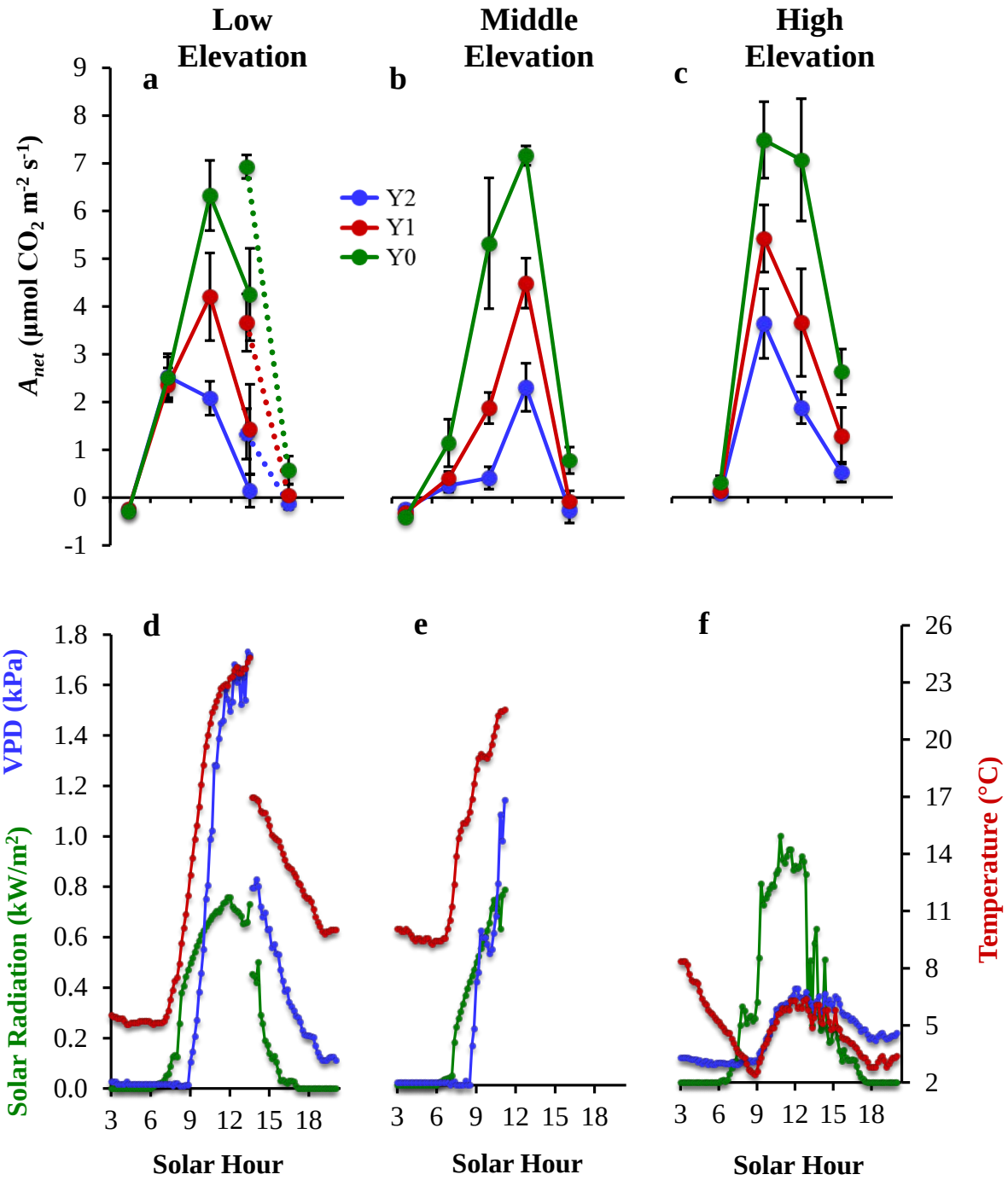

Figure 18. (a-c) Diurnal patterns of photosynthesis of Y2, Y1, and Y0 needles, and (d-f) solar radiation (green lines, left axis), VPD (blue lines, left axis), and temperature (red lines, right axis) during in October 2014. Points in a-c are means ± s.e. of 5 trees per elevation. Microclimate parameters are means of 10-min intervals sampled every 2 seconds.

Table 5. Microclimate parameters during each day of diurnal gas exchange measurements under ambient conditions in October 2014. Parameters were sampled every 2 seconds and averaged on 10-minute intervals from 3:00-20:00 solar time. Mean air temperatures and VPD are means ± s.e. of all 10-minute intervals. Weather data was incomplete at the middle elevation site, and measurements took place over 2 separate days at the low elevation site (see text).

	Low Elevation	Middle Elevation	High Elevation
Measurement Date	October 9th & 20th	October 2nd	October 4th
Mean Air Temperature (°C)	13.2 ± 0.6	-	4.8 ± 0.1
Minimum Air Temperature (°C)	5.4	-	2.4
Maximum Temperature (°C)	24.8	-	8.4
Mean VPD (kPa)	0.46 ± 0.05	-	0.19 ± 0.01
Minimum VPD (kPa)	0.01	-	0.07
Maximum VPD (kPa)	1.73	-	0.37
Evaporative Demand (kPa*h)	7.89	-	3.34
Total Insolation ($kW*h/m^{-2}$)	4.14	-	4.51

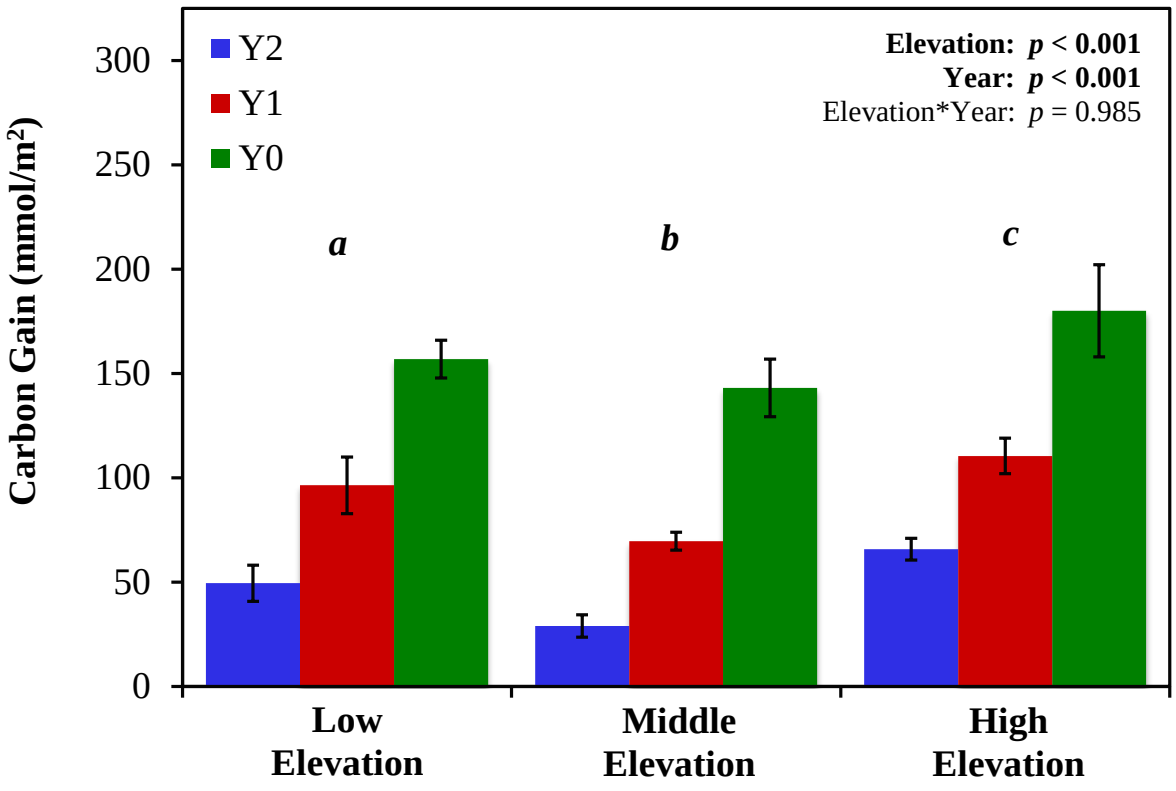

Figure 19. Daily carbon gain of Y2 (blue bars), Y1 (red bars), and Y0 (green bars) needles in October 2014. Bars are means ± s.e. of 5 trees per elevation. Letters indicate significant differences ($p < 0.05$) in daily carbon gain among elevations when all needle ages were combined per elevation.

When carbon gain of all 3 age cohorts and all 3 diurnal campaigns was combined for each tree, the effect of elevation was highly significant ($p < 0.001$, Fig. 20). Mean carbon gain was 30 % higher at high elevation than at the middle and low elevation sites, which did not differ from each other.

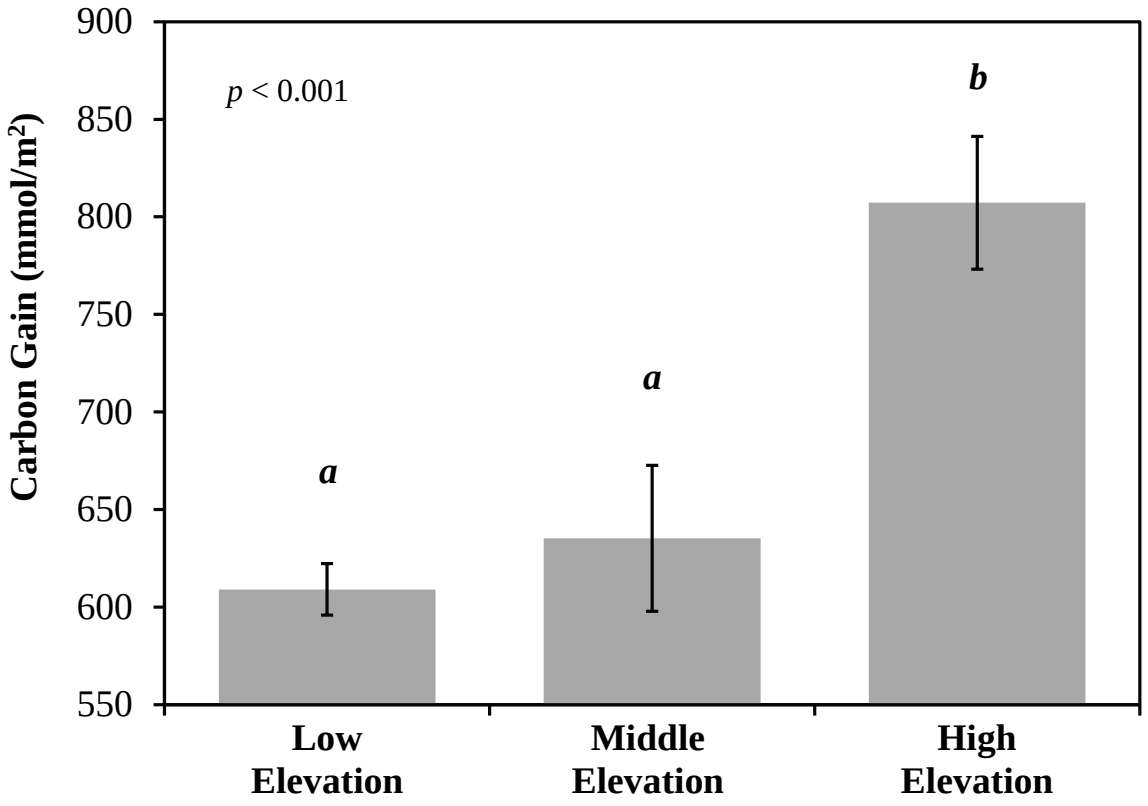

Figure 20. Total carbon gain of all needle ages and all three gas exchange campaigns combined for each tree. Bars are means ± s.e. of 5 trees per elevation. Letters indicate significant differences ($p < 0.05$) among elevations.

Photosynthesis during July 2015

In July 2015, mid-day rates of photosynthesis under ambient conditions varied among needle ages, but not among elevations (Fig. 21). Although the mean rate of photosynthesis of Y0 needles at middle and high elevation was 17% and 35% higher than at low elevation, post-hoc tests showed that the difference was marginally insignificant ($p = 0.055$). Thus, there is the suggestion of lower rates at the low elevation site. As with gas exchange measurements during the 2014 growing season, photosynthetic rates declined as needles aged

at all elevations, with rates of Y1 and Y2 needles only 51 and 20% of rates of Y0 needles, respectively.

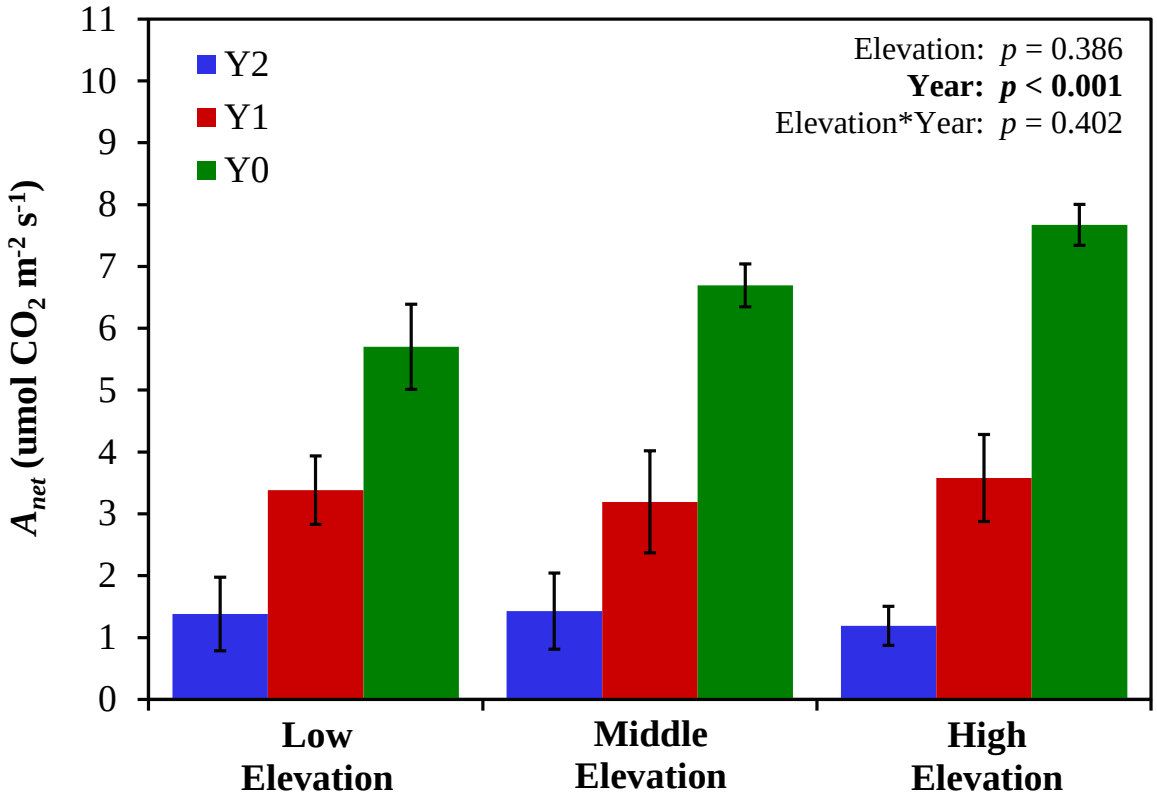

Figure 21. Mid-day photosynthesis of Y2 (blue bars), Y1 (red bars), and Y0 (green bars) needles under ambient conditions in July 2015. Bars are mean of 5 trees ± s.e.

Fv/Fm during July 2015 campaign

During July 2015, Fv/Fm was highest (0.825) for trees at the high elevation site and did not differ between the middle (0.796) and low (0.784) elevation sites (Fig. 22, $p = 0.045$).

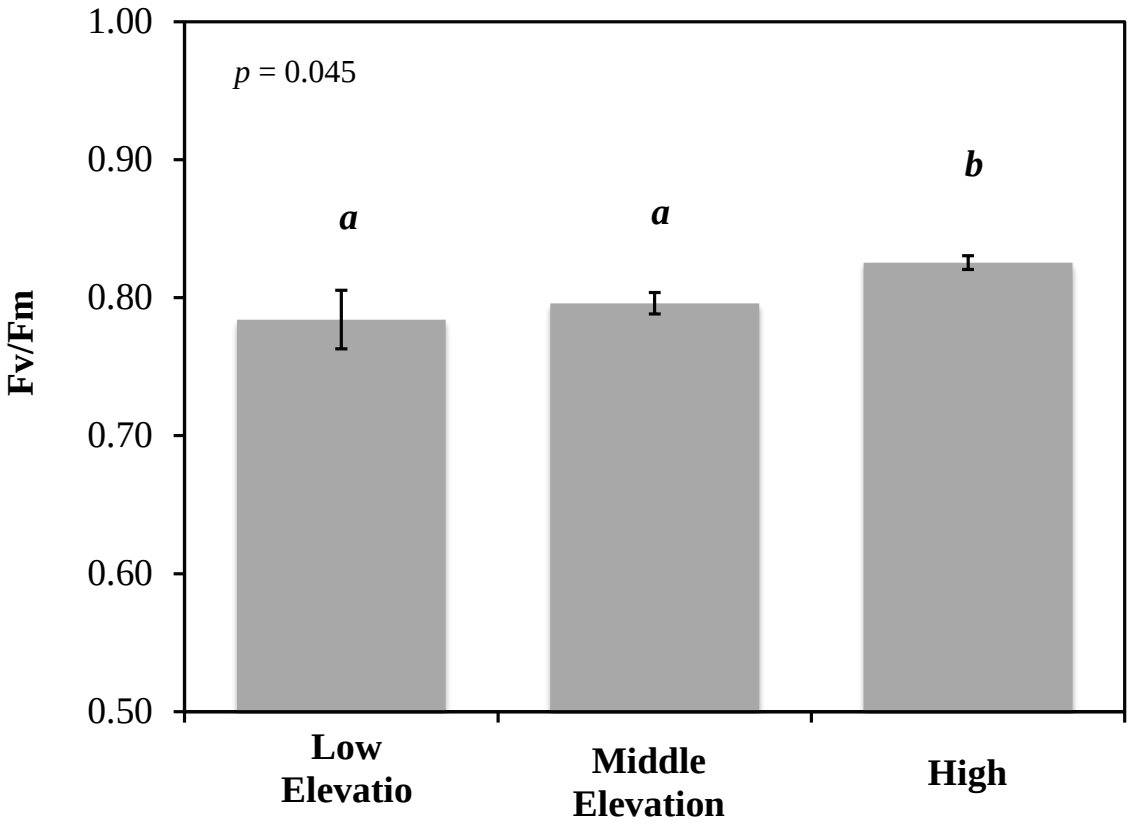

Figure 22. Mid-day Fv/Fm in July 2015. At low elevation, 4-5 measurements were averaged for each of 3 trees. At middle and high elevations, 2-3 measurements were averaged for each 5 trees. Bars are means ± s.e. of 3-5 trees per site. Letters indicate significant differences in Fv/Fm among sites.

Needle packing density (NPD)

Needle packing density (NPD) of individual shoots ranged from 17-26 needles/cm of stem length and site means ± s.e. ranged from 18.4 ± 0.7 to 22.4 ± 1.3 needles/cm stem

length. An ANOVA showed that variation among all sites was significant ($p = 0.0264$, $n = 5$ trees/site), although post-hoc tests indicated that pairwise differences were significant between only the 710 m and 1228 m sites, and not between the two sites within each of the elevation categories (Fig. 23). Subsequently, mean NPDs of each site were used as replicates in linear regression, which showed that elevational trends were not significant ($p = 0.6855$, $r^2 = 0.0453$).

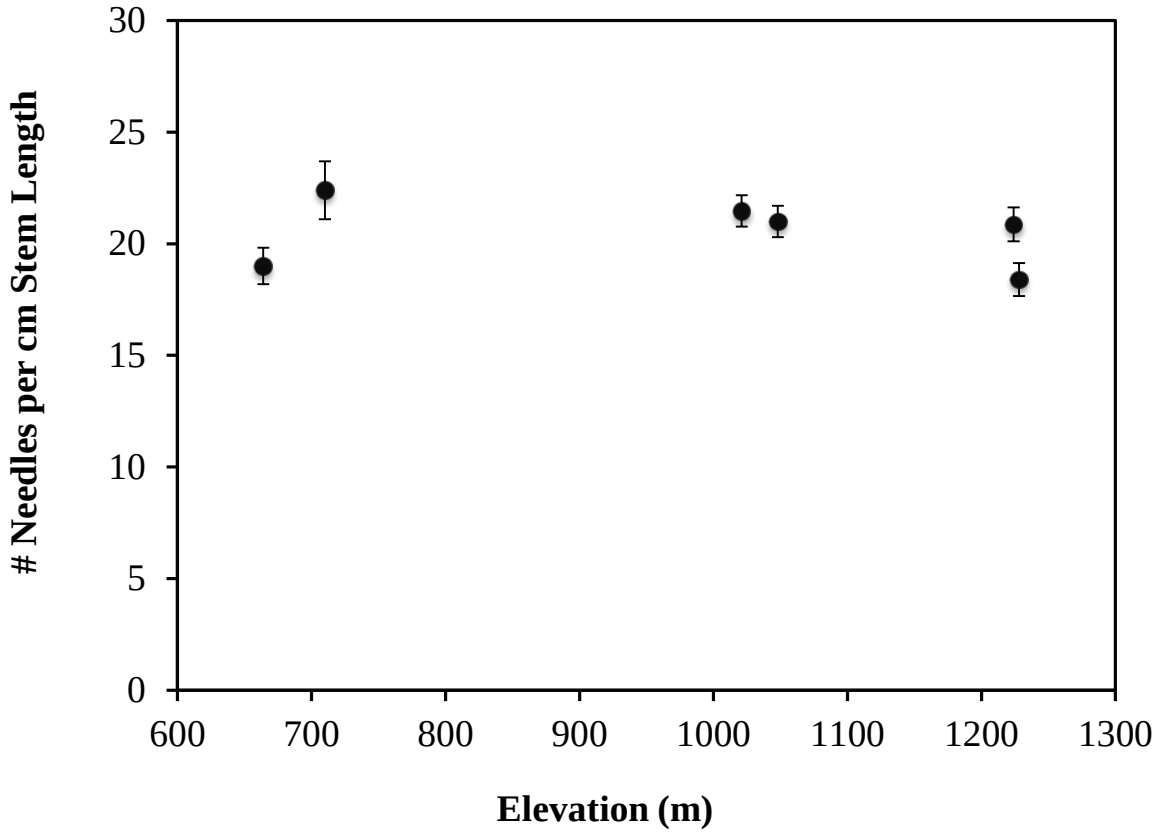

Figure 23. Needle packing density (number of needles per linear cm of stem) as a function of elevation. Points are means ± s.e. of 5 stems per site.

Diurnal Patterns of Silhouette to Projected Needle Area Ratio (SPAR)

SPAR values were determined for south-facing branches on the same trees for which gas exchange measurements were conducted and showed no differences among elevations (Fig. 24), although for all but one time during the day, SPAR appeared lower for high elevation trees, even though this was never statistically significant. SPAR was lowest early in the morning and the late afternoon, and peaked at or just after solar noon.

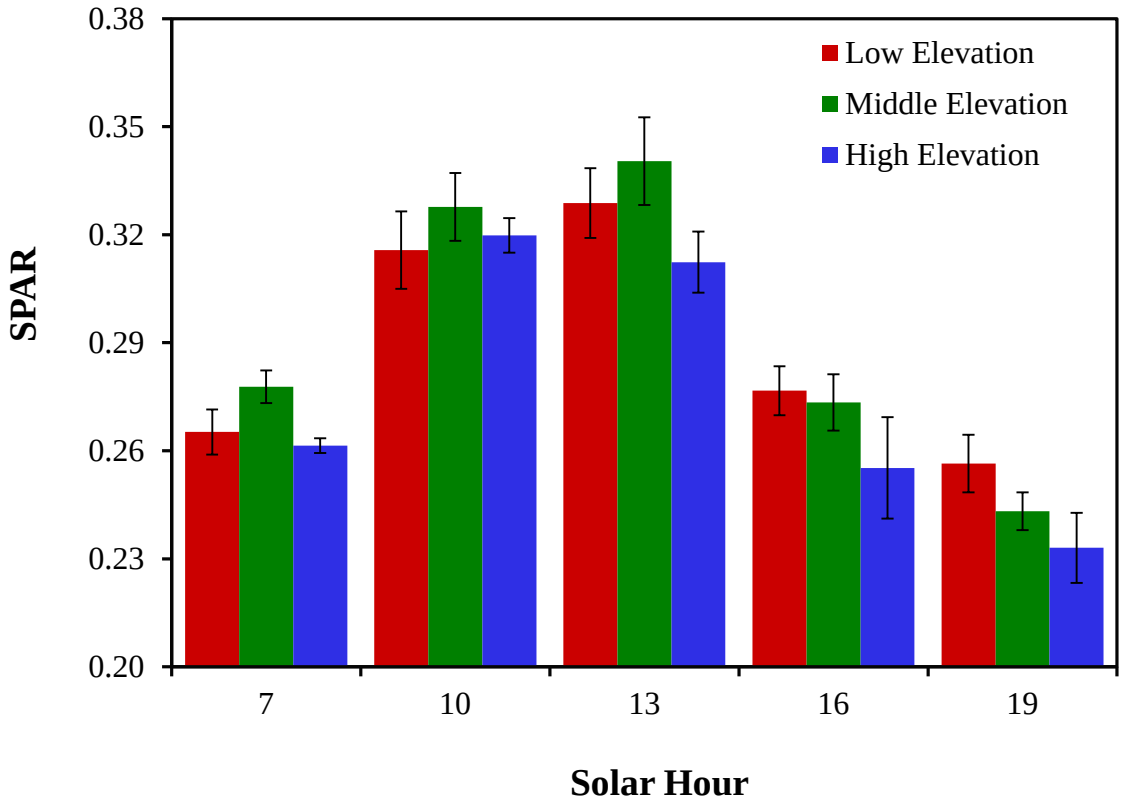

Figure 24. Diurnal patterns of silhouette-to-projected area ratios among elevations. SPAR was determined for Y2, Y1, and Y0 shoots during June, July, and October and then averaged per tree. Bars are means ± s.e. of 5 trees per elevation.

Specific Needle Mass (SNM)

Specific needle mass (dry mass per unit projected needle area) ranged from 0.0124 to 0.0239 g/cm^2 and was equivalent among elevations (p = 0.058) but increased as needles aged (p < 0.001, Fig. 25). SNM of Y1 needles was 12% higher than that of Y0 needles, Y2 needles were 26% higher than Y1 (p < 0.0001), and effects of needle age were consistent at each elevation.

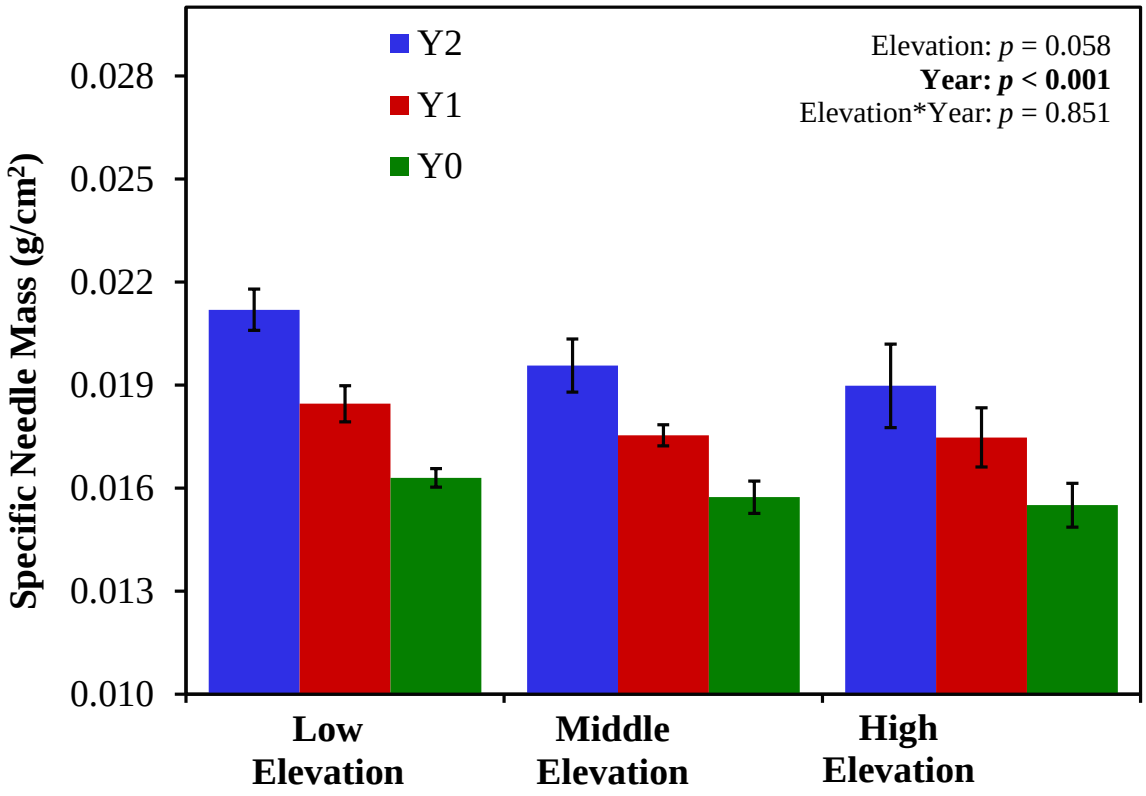

Figure 25. Specific needle mass (dry needle mass per unit projected needle area) of Y2, Y1, and Y0 needles. SNM was determined for each needle age during June, July, and October 2014 and then averaged for each tree. Bars are means ± s.e. of 5 trees per elevation.

Discussion

Microclimate

Topography differed among the sites where weather stations were located, which explains why several microclimatic variables did not match expected trends. The low elevation site was near the bottom of a hill that extends ~75 m above the study site and weather station location, and the middle elevation site was in a valley with nearby hills extending ~75 m above and a nearby ridgeline extending ~200 m above the study site and weather stations. However, the topography was quite different at the high elevation site, which was at the top of a peak rising ~500 m above the surrounding landscape. High exposure at this site caused higher daily maxima and higher average wind speeds than at the middle and low elevation sites. Here, temperatures typically increased shortly after sunrise, whereas at both the low and middle elevation sites, temperatures and VPDs often continued to decrease for 1-2 hours after sunrise because cold air and fog from nearby higher land descended into the valleys and remained for several hours. These inversions were most common at the middle elevation site, but occurred occasionally at the low elevation site too. Although daily maximum temperatures matched expected trends for a moist adiabatic lapse rate, the daily minimum air temperatures and mean and minimum VPDs (and their integration, daily evaporative demand) were lowest at the middle elevation site due to this frequent cold-air drainage and inversion. Despite the departure from expectations for these parameters, our elevational gradient design can still be considered an appropriate surrogate for climate warming because mean and maximum air temperatures, mean and maximum VPDs, and integrated evaporative demand at the low elevation site were higher than at the middle and high elevation sites.

Cloud events (either cloudiness or cloud-immersion) play a key role in shaping microclimate along an elevational gradient. Water droplets scatter and reflect sunlight which reduces radiation at the canopy (Urban et al. 2007). Although the presence of clouds was not monitored directly, mean solar radiation and integrated insolation increased as elevation decreased in this study, suggesting a decrease in the frequency of cloud events at lower elevations. Although clouds reduce irradiance of all wavelengths, they increase the relative proportion of diffuse to direct sunlight (Reinhardt et al. 2010). Since Fraser fir has 3-dimensional needles arranged radially about their stems and a complex shoot structure, they can efficiently utilize this diffuse light (Berry and Smith 2013). Clouds also reduce ambient temperatures and evaporative demand compared to sunny days (Berry and Smith 2012, Reinhardt and Smith 2008a), so the decrease in their frequency at lower elevations amplifies the effects of warming due to adiabatic lapse.

Bud-break

Synchronizing the timing of bud-break with seasonal weather patterns allows plants to maximize their utilization of the growing season and to minimize freezing injury due to low temperatures. Although to the best of my knowledge there have been no studies on those factors controlling bud-break in Fraser fir, the primary factors that have been suggested to control bud-break in other tree species are (1) photoperiod, (2) early-spring temperatures, and (3) the degree of winter chilling (Campbell and Sugano 1975, Körner and Basler 2010). As climate change progresses, warm temperatures will occur earlier in the spring, when photoperiods are shorter. The ability of a species to take advantage of these warmer temperatures, longer growing season, and higher soil moisture in the spring will depend

heavily on whether the species relies on photoperiod for its bud-burst cues, or temperature, or some combination thereof. For a plant to shift the timing of bud-break to better match early-spring temperatures and maximize the length of the growing season, its buds must be sensitive to spring temperatures, and either (1) not be sensitive to photoperiod and/or winter chilling, or (2) have photoperiod and/or winter chilling requirements that, once achieved, allow buds to respond to early spring temperatures.

Several studies have shown that warming in the spring is the primary cue for bud-break in early- and mid-successional species. However, bud-break in long-lived, late-successional species is controlled by both winter chilling and photoperiod, and complex interactions exist between these two environmental cues (Körner and Basler 2010, Kolářová et al. 2014). Basler and Körner (2012) showed that bud-break in *Abies alba* and *Picea abies* is highly sensitive to photoperiod, with shorter photoperiods delaying bud-burst. Similarly, Royce and Barbour (2001) found that bud-burst in *A. concolor* and *A. magnifica* is tightly regulated by photoperiod, provided that a minimum temperature threshold has been surpassed (minimum daily temperatures >2-3 °C). However, since our study sites were at approximately the same latitude (< 15 km range from north-south), photoperiod did not differ among sites, and so could not account for variation in phenology.

Previous studies have shown that winter-chilling affects bud-burst in a variety of conifers. With warming, exposure to winter chilling will decrease, so species that depend upon reaching a critical level of chilling degree days before buds can be released from dormancy will have delayed bud-burst. Partanen et al. (1998) exposed *P. abies* seedlings to varying amounts of winter chilling, and found that greater winter chilling caused buds to emerge sooner, suggesting physiological changes occur during winter and that a vernalization

requirement must be met. Chilling requirements have also been demonstrated in four *Pinus spp*., with long, cold winters advancing phenology compared to warmer or shorter winters. Spring phenology was found to be more heavily influenced by winter temperatures than by early spring temperatures (Clark et al. 2014).

Although our weather stations were not installed early enough to record microclimate in winter and early spring, it is fair to assume that trends during those periods would be similar to trends from May 25th – October 31st reported in this study. Therefore, we can assume that trees were exposed to more winter chilling at high elevations than at low elevations. However, if winter chilling was the only factor dictating bud-burst in Fraser fir, then bud-burst would have occurred sooner at high elevations than at low elevations. Therefore, it is likely that, if there are winter chilling and/or photoperiod requirements for bud-break in Fraser fir, then these requirements were met along the entire elevational gradient in this study and the earlier bud-burst observed at low elevations resulted from the warmer early spring temperatures there.

Weather in the high-elevation peaks of the Southern Appalachians is somewhat unpredictable from year to year (Richardson et al. 2004), and can occasionally include injurious late-spring frosts. In fact, given how some trees cue on photoperiod, such late spring frosts can induce severe damage to trees that break buds during these times (Emerson et al. 2008, Augspurger 2013). Native populations of Fraser fir have probably adapted bud-break strategies to best exploit their relatively short growing season at elevations above 1500 m and to avoid injury due to late-spring frosts. Their strategy is likely based on spring temperatures rather than photoperiod or winter chilling, since photoperiod does not vary among years and winter chilling is a poor predictor of temperatures the following spring,

although no studies have investigated this in Fraser fir with experimental manipulation of these factors. Since Christmas tree genotypes are selected from local native populations, then bud-break in Christmas tree farms is probably controlled by the same factors that control bud-break in the native populations.

Worrall (1983) found that date of bud-burst can vary year-to-year by up 5 weeks in *A. amabilis* and *A. lasiocarpa*, owing to differences in both heat-sum and temperature threshold values among years. Additionally, bud-burst occurred ~4 weeks later in native populations at high-elevation peaks, based on anecdotal observations, than in the commercial Christmas tree range. This further supports the explanation that neither photoperiod nor winter chilling are the primary controls of bud-break in Fraser fir, again suggesting that spring temperatures are the primary microclimatic factor.

Shoot Growth

Shoot length in conifers is determinate, such that the final length is determined at the start of the growing season (Royce and Barbour 2001). However, high temperatures and/or drought, and subsequent low water potentials and turgor loss, can cause early cessation of growth in the fall (Cannell et al. 1976, Junttila 1986, Green 2007). In this study, final shoot lengths did not vary as a function of elevation, suggesting that drought was not severe enough to cause early cessation of shoot expansion. Though elevational trends in final shoot lengths were not significant, variation between sites at of each elevation category is possibly due to agricultural practices such as shearing during the previous growing season, or due to differences in topography among sites.

The shift in timing and rate of expansion among elevations was remarkable. At low elevations, shoots began expanding sooner, and reached their final lengths sooner, than at middle and high elevations. This earlier shoot expansion is partially attributable to earlier bud-break at low elevations, since shoot extension begins once complete bud-burst is achieved, but temperature likely also plays a key role in governing the subsequent rate of shoot expansion. A minimum temperature threshold has been reported for the initiation of shoot growth in trees (Campbell and Sugano 1975, Green 2007), and this likely occurred earlier at low elevations in my study. The continued higher temperatures throughout the spring would contribute to the faster elongation rates observed, and also perhaps to the earlier cessation of elongation as reported in this study.

Although earlier bud-break and shoot expansion will advance the beginning of the growing season, the earlier cessation of growth means that the total length of the shoot extension period was fairly similar across elevations. Thus, in this species, warming may shift the shoot extension period to earlier in the season, but it does not lengthen it. This has potential consequences for seasonal carbon gain. First, earlier extension means that the current cohort of needles (Y0) may mature earlier and thus become photosynthetically competent before trees at middle and high elevations. They could then potentially take advantage of early season cool temperatures and higher soil moisture to carry on high rates of photosynthesis without being subject to great atmospheric evaporative demand and possible drought stress that may occur later on in the season. Second, the failure of shoot lengths to differ among elevations, as also found for needle packing density, SPAR, and SNM, means that warming will most likely not alter these aspects of tree architecture and canopy development and light capture will probably not change as trees grow in warmer climates.

Thus warming will probably exert its effects more through physiological adjustments at the shoot and cellular levels then through alterations in canopy architecture.

Although phenological adjustment of trees at low elevations to take advantage of early season warming could potentially lead to greater carbon gain throughout the year, there are risks to such behavior. First, advancing phenology leads to increased risk of late-spring frost damage (Murray et al. 1994, Augspurger 2013). In addition, shoots that emerge earlier in the year will experience lower cumulative daily PPFD via shorter photoperiods and a lower angle of incidence of the sun, such that the potential gain may not be as much as first thought. Consequently, net photosynthesis may not increase as much compared to shoots that emerge later. Furthermore, since dark respiration increases with temperature (Yamori et al. 2014) dark respiration rates may be lower in the early spring due to cooler temperatures, which would favor greater carbon assimilation in the spring compared to the summer, when temperatures are much higher.

Trunk Growth

Timing and magnitude of trunk growth throughout a growing season is a function of the length of the growing season, the number of tracheids produced each year, lumen diameter of those tracheids, and thickness of their cell walls (Beedlow et al. 2013). Each of these factors are controlled by a complex interaction of several physiological and microclimatic conditions including stored carbohydrates from the previous season, early spring temperatures that signal the release of cambium cells from dormancy, and water availability in both the early spring and throughout the growing season. In this study, total trunk growth (expressed as % increase) was highest at middle elevations, implying that trunk

growth in Fraser fir is influenced by a complex interaction of several microclimatic conditions, and suggesting a threshold elevation where the benefit of warm temperatures early in the season is surpassed by the detriment of increasing evaporative demand. This explanation is consistent with Sidor et al. (2015), who found that trunk growth in *P. abies* is limited by summer temperatures at high elevations, but summer precipitation and water availability limits growth at low elevations.

Trends in the timing of trunk growth imply that the length of the growing season increases as elevation decreases. In this study, the duration of trunk growth was longest at low elevations, with trees reaching various proportions of their total growth much later than at middle and high elevations. This pattern is consistent with the findings of other studies. Rossi et al. (2011) showed that growing season length is coupled with warm air temperatures, and produced a model showing that the annual duration of cambium growth increases by 8-11 days per each 1°C increase. Lenz et al. (2013) found that timing of trunk and shoot xylogenesis is decoupled from shoot growth (which is limited by bud-break), and highly coupled to warm air temperatures irrespective of soil temperatures, particularly early in the spring. Cambium reactivation occurs very early in the spring, and warm temperatures during this period can lead to wider cambial zones, resulting in wider tree rings over the entire growing season. Rossi et al. (2011) found that warm air temperatures increase the number of tracheids produced early in the season in *P. mariana*, which could potentially lead to more trunk growth throughout the season unless warm air temperatures and subsequent water stress limit growth. Therefore, trunk growth in this study may have been limited by high temperatures at low elevations, but by a shorter growing season and cooler temperatures at high elevations.

Photosynthetic capacity

There were no elevational trends in gas exchange under standard conditions. Although foliar nitrogen content was slightly lower at the high elevation sites (but only by 0.2%), and photosynthetic pigments and proteins account for the majority of leaf nitrogen (Evans 1989), this difference was probably not biologically important, especially because photosynthetic rates under standardized conditions were equivalent among elevations. This implies that photosynthetic capacity was essentially identical among trees from different elevations when chamber conditions were controlled, supporting the use of the elevational gradient design in drawing conclusions about carbon gain under ambient conditions in this study. It also shows that the physiological tolerance of this species is quite large, since trees were able to perform the same despite growing along an elevational gradient that spans over 564 m. Agricultural research of Fraser fir Christmas trees has shown that tripling the amount of nitrogen fertilization increases foliar nitrogen content by less than 0.2 percentage points (Hinesley et al. 2000), further supporting the explanation that nitrogen availability is not limiting photosynthetic capacity.

The reduction of intrinsic photosynthetic capacity and respiration in older needles is well documented in other fast-growing conifer species. Freeland (1952) found that maximum photosynthetic capacity occurs shortly after needle maturation during the first growing season in several *Pinus*, *Abies*, and *Picea* species. Similarly, Zhou et al. (2011) reported that light-saturated photosynthetic rates were higher in current-year needles than one-year-old needles of *Pinus sylvestriformis.*

Gas Exchange Under Ambient Conditions

The response of gas exchange under ambient conditions to microclimatic stressors was most remarkable during the first campaign, in June 2014. Maximum temperatures and VPDs on each date of gas exchange measurements were much higher at low elevation than at middle and high elevation (see Table 3). The extremely high temperatures and evaporative demand at low elevation caused greater plant moisture stress (see Lauren Wood 2016, in preparation). Mid-day water potentials were -1.32, -1.0, and -0.8 MPa at low, middle, and high elevations, respectively while mid-day stomatal conductances were 0.024, 0.072, and 0.068 mol H_2O m^{-2} s^{-1}, respectively. These dramatic physiological responses at low elevation suggest that high temperatures and VPDs can severely reduce gas exchange rates in Fraser fir Christmas trees.

These unusually high temperatures and VPDs did not occur during the July and October gas exchange campaigns. During the October campaign, temperatures at high elevation plunged to 2.4 °C in the morning and remained ≤ 8.4 °C throughout the day, but temperatures at low elevation climbed to 24.8 °C. Although we've shown that exceptionally high temperatures (>30 °C during the June campaign) can reduce gas exchange rates, fairly low temperatures seem to have no negative effects, suggesting that Fraser fir Christmas trees can maintain high levels of physiological activity across a wide range of temperatures up to a certain point, although exceptionally hot days are detrimental. Maintenance of high photosynthetic rates in the face of low temperatures makes sense when one considers that the natural range of this species is > 1,500 m, where such temperatures would be encountered quite frequently, especially early and later in the growing season. If the climate warms by 3.6 °C over the next century as predicted (IPCC 2013), and if extreme weather events such as

days with unusually high temperatures or VPDs become more common, then low elevation Christmas tree farms that are already beginning to experience detrimental effects of high temperatures may experience decreased productivity, as well as disease resistance, and this could make commercial production unviable at these locations. Conversely, trees in middle to high elevation farms would benefit from a longer growing season. However, there is much less land available for commercial growing at high than middle or low elevations, and if the industry moves upslope, there may be a consolidation in the number of farms and a reduction in their mean size.

NPD

Shoot-level architectural characteristics such as needle packing density and radial arrangement of needles around a stem are known to be highly plastic in conifers, and the arrangement of needles on the stem can influence leaf temperatures, self-shading, and photosynthetic rates at both the shoot and needle levels. Smith and Carter (1988) found that in *P. engelmannii*, *A. lasiocarpa*, and *P. contorta*, greater needle packing increased needle temperatures due to increased boundary layer thickness, increased rates of photosynthesis per shoot, but decreased rates of photosynthesis per needle due to self-shading. In this study, needle packing density was highly variable among trees within a site, and even among shoots within a tree (based on anecdotal observations). However, it did not vary significantly with elevation, suggesting that while this trait may be plastic, the temperatures or water stress encountered in this study were not sufficient to cause any measurable changes.

SPAR

The silhouette area represents the total area intercepting direct-beam sunlight, which changes diurnally and seasonally for any particular shoot (Sprugel et al. 1996, Robakowski et al. 2003). The projected leaf area, on the other hand, represents the area intercepting light normal to the needles when they are removed from their stems (Smith et al. 1991). It can be thought of as better representing the intrinsic photosynthetic capacity minus the confounding effects of shoot geometry and architecture. The ratio of silhouette to projected leaf areas (SPAR) is a measure of self-shading, and is a function of the density of needle packing, needle size and geometry, radial arrangement of needles around the stem, and shoot inclination. Lower SPAR indicates higher self-shading and could be adaptive by diminishing the negative effects of high sunlight and increasing light levels deeper in the canopy, while a higher SPAR reflects greater light-interception efficiency in shade-grown shoots or stressed trees (Ishii et al. 2012).

In this study, there were no apparent elevational trends in SPAR, suggesting that microclimatic conditions along the elevational gradient, and subsequent plant stress, were not sufficient to cause architectural adjustments. However, SPAR did vary by time of day at all sites, reaching a maximum (least self-shading) near solar noon and decreasing later in the day. Since maximum solar radiation occurs at solar noon, but daily maximum temperatures and VPD occur after solar noon, the diurnal patterns of SPAR in this study could be a modification to increase water use efficiency. High SPAR (low self-shading) at solar noon maximizes light-interception earlier in the day when temperatures and VPD are lower. Although leaf temperatures were not directly measured in this study, lower SPAR (more self-shading) in the afternoon would minimize increases in leaf temperatures, and subsequently

reduce leaf-to-air water vapor pressure deficit and water loss, when evaporative demand is the greatest. That this ratio was invariant across elevations, and that photosynthesis generally peaked earlier at lower elevations, suggests that trees at low elevations may benefit from this increase in water use efficiency more so than trees at middle or high elevations, since trees at the latter two sites have peak carbon gain later in the day.

SNM

Specific needle mass represents the ratio of dry needle mass to projected area, and is known to be highly plastic in response to temperature, light, and moisture availability (Boyce 1993, (Chen et al. 1996, Poulos and Berlyn 2007). It is important to note that since SNM is a ratio, it confounds needle density (mass per unit volume) and needle geometry (thickness, Witkowski and Lamont 1991). Although increasing SNM might increase water use efficiency by reducing the ratio of surface area to volume, SNM was equivalent among elevations in this study, suggesting that water stress was not extreme enough to cause needle-level adjustments in this trait.

SNM increased as needles aged as has been reported for other conifer species (Zhou et al. 2011, Jensen et al. 2015). Additional analyses (not shown) indicated that this was driven by an increase in mass as needles aged, and that needle area did not significantly change after needles were formed. A potential explanation is that older needles may be used to store non-structural carbohydrates (NSC), although we did not investigate NSCs in this study, or that as needles age, carbon is put into cell walls, making the needles heavier.

Conclusion

We found that Fraser fir Christmas trees generally tolerate the higher temperatures and evaporative demand at low elevation Christmas tree farms, despite growing as much as 1000 m lower than their native range. The shift in timing of the growing season was remarkable, with trees at low elevations displaying an earlier onset and later cessation of growth, although differences in trends of total shoot and trunk diameter growth throughout the season were mostly negligible among elevations. This suggests that the costs of higher mid-season temperatures at low elevations may be offset by the benefits of a longer growing season, with trees at low elevation taking advantage of lower evaporative demand and cooler temperatures in the spring. Leaf- and shoot-level architectural characteristics did not vary along the elevational gradient, suggesting that environmental stressors are not currently extreme enough to cause adjustments in these traits. Gas exchange rates under standard conditions were equivalent among elevations, and measurements under ambient conditions confirmed that high photosynthetic rates are maintained across a wide range of temperatures, although exceptionally high temperatures in June drastically reduced carbon gain throughout the day for trees at low elevation.

If climate change progresses as predicted, including higher cloud ceilings, increased evaporative demand, and higher temperatures (projected increase of 3.6 °C over the next century, IPCC 2013), then low and middle elevation Christmas tree farms may experience even greater stress, which could result in decreased productivity, potentially making commercial production unviable at these locations. Conversely, trees at high elevation farms would benefit from a longer growing season. Although these trees appear to be quite robust and seem to thrive until harvest age, at least under current environmental conditions, there is

much less land available for commercial growing at high than middle or low elevations, and if the industry moves upslope in the future, there may be a consolidation in the number of farms, a reduction in their mean size and less production.

References

Arnold RJ, Jett JB, McKeand SE (1994) Natural variation and genetic parameters in Fraser fir for growth and Christmas tree traits. Can J For Res 24:1480-1486.

Augspurger C (2013) Reconstructing patterns of temperature, phenology, and frost damage over 124 years: Spring damage risk is increasing. Ecology 94:41-50.

Basler D, Körner C (2012) Photoperiod sensitivity of bud burst in 14 temperate forest tree species. Agric For Meterol 165:73-81.

Beedlow PA, Lee EH, Tingey DT, Waschmann RS, Burdick CA (2013) The importance of seasonal temperature and moisture patterns on growth of Douglas-fir in western Oregon, USA. Agric For Meteorol 169:174-185.

Berry ZC, Hughes NM, Smith WK (2013) Cloud immersion: an important water source for spruce and fir saplings in the southern Appalachian Mountains. Oecologia 174:319-326.

Berry ZC, Smith WK (2012) Cloud pattern and water relations in *Picea rubens* and *Abies fraseri*, southern Appalachian Mountains, USA. Agr For Met 162:27-34.

Berry ZC, Smith WK (2013) Ecophysiological importance of cloud immersion in a relic spruce-fir forest at elevational limits, southern Appalachian Mountains, USA. Oecologia 173:637-648.

Berry ZC, Smith WK (2014) Experimental cloud immersion and foliar water uptake in saplings of *Abies fraseri* and *Picea rubens*. Trees 28:115-123.

Berry ZC, White JC, Smith WK (2014) Foliar uptake, carbon fluxes and water status are affected by the timing of daily fog in saplings from a threatened cloud forest. Tree Physiol 34:459-470.

Bolstad PV, Swift L, Collins F, Réginère J (1998) Measured and predicted air temperatures at basin to regional scales in the southern Appalachian mountains. Agric For Meteorol 91:161-176.

Boyce RL (1993) A comparison of red spruce and balsam fir shoot structures. Tree Physiol 12:217-230.

Campbell R, Sugano A (1975) Phenology of bud burst in Douglas-Fir related to provenance, photoperiod, chilling, and flushing temperature. Bot Gazette 136:290-298.

Cannell M, Thompson S, Lines R (1976) An analysis of inherent differences in shoot growth within some north temperature conifers. In: Cannell M, Last F (eds) Tree Physiology and Yield Improvement. Academic Press, London, UK, pp: 173-205.

Chen HY, Klinka K, Kayahara GJ (1996) Effects of light on growth, crown architecture, and specific leaf area for naturally established *Pinus contorta* var. *latifoli*a and *Pseudotsuga menziesii* var. *glauca* saplings. Can J For Res 26:1149-1157.

Clark J, Melillo J, Mohan J, Salk C (2014) The seasonal timing of warming that controls onset of the growing season. Glob Change Biol 20:1136-1145.

Cordell S, Goldstein G, Mueller-Dombois D, Webb D, Vitousek PM (1998) Physiological and morphological variation in *Metrosideros polymorpha*, a dominant Hawaiian tree species, along an altitudinal gradient: the rolle of phenotypic plasticity. Oecologia 113:188-196.

Emerson JL, Frampton J, McKeand SE (2006) Genetic variation of spring frost damage in 3-year-old Fraser fir Christmas tree plantations. HortScience 41:1531-1536.

Emerson JL, Frampton J, McKeand SE (2008) Genetic gariation in early growth and bud production among natural populations of Fraser fir. HortScience 43: 661-666.

Evans JR (1989) Photosynthesis and nitrogen relationships in leaves of C3 plants. Oecologia 78:9-19.

Freeland RO (1952) Effect of age of leaves upon the rate of photosynthesis in some conifers. Plant Physiol 27:685-690.

Fryer J, Ledig F (1972) Microevolution of the photosynthetic temperature optimum in relation to the elevational complex gradient. Can J Bot 50:1231-1235.

Gebhardt T, Häberle K-H, Matyssek R, Schulz C, Ammer C (2014) The more, the better? Water relations of Norway spruce stands after progressive thinning. Agric For Meteorol 197:235-243.

Green D (2007) Controls of growth phenology vary in seedlings of three, co-occurring ecologically distinct northern conifers. Tree Physiol 27:1197-1205.

Hinesley LE, Derby SA (2004) Growth of Fraser fir Christmas trees in response to annual shearing. HortScience 39:1644-1646.

Hinesley LE, Snelling LK (1997) Basal pruning Fraser fir Christmas trees. HortScience 32:324-326.

Hinesley LE, Snelling LK, Campbell CR, Roten DK, Hartzog J (2000) Nitrogen increases fresh weight and retail value of Fraser fir Christmas trees. HortScience 35:860-862.

Hinesley LE, Wright RD (1989) Biomass and nutrient accumulation in Fraser-fir Christmas trees. HortScience 24:280-282.

IPCC (2013) Climate Change 2013: The Physical Science Basis. IPCC, Geneva, Switzerland.

Ishii H, Ford ED, Boscolo ME, Manriquez AC, Wilson ME, Hinckley TM (2002) Variation in specific needle area of old-growth Douglas-fir in relation to needle age, within-crown position and epicormic shoot production. Tree Physiol 22:31-40.

Ishii H, Hamada Y, Utsugi H (2012) Variation in light-intercepting area and photosynthetic rate of sun and shade shoots of two *Picea* species in relation to the angle of incoming light. Tree Physiol 32:1227-1236.

Jensen AM, Warren JM, Hanson PJ, Childs J, Wullschleger SD (2015) Needle age and season influence photosynthetic temperature response and total annual carbon uptake in mature *Picea mariana* trees. Ann Bot 116:821-832.

Johnson DM, Smith WK (2006) Low clouds and cloud immersion enhance photosynthesis in understory species of a southern Appalachian spruce-fir forest (USA). Am J Bot 93:1625-1632.

Junttila O (1986) Effects of temperature on shoot growth in northern provenances of *Pinus sylvestris* L. Tree Physiol 1:185-192.

King GM, Gugerli F, Fonti P, Frank DC (2013) Tree growth response along an elevational gradient: climate or genetics? Oecologia 173:1587-1600.

Kolářová E, Nekovář J, Adamík P (2014) Long-term temporal changes in central European tree phenology (1946-2010) confirm the recent extension of growing seasons. Int J Biometeorol 58:1739-1748.

Körner C, Basler D (2010) Phenology under global warming. Science 327:1461-1462.

Kulaç Ş, Nzokou P, Guney D, Cregg BM, Turna I (2012) Growth and physiological response of Fraser fir [*Abies fraseri* (Pursh) Poir.] seedlings to water stress: seasonal and diurnal variations in photosynthetic pigments and carbohydrate concentration. HortScience 47:1512-1519.

Kunkel KE, Stevens LE, Stevens SE, Sun L, Janssen E, Wuebbles D, Konrad II CM, Fuhman CM, Keim BD, Kruk MC, Billet A, Needham H, Schafer M, Dobson JG (2013) Regional Climate Trends and Scenarios for the U.S. National Climate Assessment. Part 2. Climate of the Southeast U.S., NOAA Technical Report NEDIS 142-2.

Laseter SH, Ford CR, Vose JM, Swift LW, Jr (2012) Long-term temperature and precipitation trends at the Coweeta Hydrologic Laboratory, Otto, North Carolina, USA. Hydrol Res 43:890-901.

Lenz A, Hoch G, Körner C (2013) Early season temperature controls cambial activity and total tree ring width at the alpine treeline. Plant Ecol Divers 6:365-375.

Liesch PJ, Williamson RC (2010) Evaluation of chemical controls and entomopathogenic nematodes for control of *Phyllophaga* white grubs in a Fraser fir production field. J Econ Entomol 103:1979-1987.

Murray M, Smith R, Leith I, Fowler D, Lee H, Friend A, Jarvis P (1994) Effects of elevated CO_2, nutrition and climatic warming on bud phenology in Sitka spruce (*Picea sitchensis*) and their impact on the risk of frost damage. Tree Physiol 14:691-706.

Nodvin SC, Van Miegroet H, Lindberg SE, Nicholas NS, Johnson DW (1995) Acidic deposition, ecosystem processes, and nitrogen saturation in a high elevation southern Appalachian watershed. Water Air Soil Poll 85:1647-1652.

North Carolina Cooperative Extension Service. North Carolina Christmas trees by the numbers. https://christmastrees.ces.ncsu.edu/christmastrees-nc-christmas-trees-by-the-numbers (3 Dec 2015, date last accessed).

Nzokou P, Cregg BM (2010a) Growth, biomass, and nitrogen use efficiency of containerized Fraser fir (*Abies fraseri*) as related to irrigation and nitrogen fertilization. HortScience 45:946-951.

Nzokou P, Cregg BM (2010b) Morphology and foliar chemistry of containerized *Abies fraseri* (Pursh) Poir. seedlings as affected by water availability and nutrition. Ann For Sci 67:602.

Partanen J, Koski V, Hänninen H (1998) Effects of photoperiod and temperature on the timing of bud burst in Norway spruce (*Picea abies*). Tree Physiol 18:811-816.

Potter KM, Frampton J, Josserand SA, Nelson CD (2008) Genetic variation and population structure in Fraser fir (*Abies fraseri*): a microsatellite assessment of young trees. Can J For Res 38:2128-2137.

Poulos HM, Berlyn GP (2007) Variability in needle morphology and water status of *Pinus cembroides* across an elevational gradient in the Davis Mountains of west Texas, USA. J Torrey Bot Soc 134:281-288.

Reinhardt K, Castanha C, Germino MJ, Kueppers LM (2011) Ecophysiological variation in two provenances of *Pinus flexilis* seedlings across an elevation gradient from forest to alpine. Tree Physiol 31:615-625.

Reinhardt K, Smith WK (2008a) Impacts of cloud immersion on microclimate, photosynthesis and water relations of *Abies fraseri* (Pursh.) Poiret in a temperate mountain cloud forest. Oecologia 158:229-238.

Reinhardt K, Smith WK (2008b) Leaf gas exchange of understory spruce-fir saplings in relict cloud forests, southern Appalachian Mountains, USA. Tree Physiol 28:113-122.

Reinhardt K, Smith WK, Carter GA (2010) Clouds and cloud immersion alter photosynthetic light quality in a temperate mountain cloud forest. Botany 88:462-470.

Richardson AD, Berlyn GP (2002) Spectral reflectance of *Betula papyrifera* (Betulaceae) Leaves along an elevational gradient on Mt. Mansfield, Vermont, USA. Am J Bot 89:88-94.

Richardson AD, Berlyn GP, Gregoire TG (2001) Spectral reflectance of *Picea rubens* (Pinaceae) and *Abies balsamea* (Pinaceae) needles along an elevational gradient, Mt. Moosilauke, New Hampshire, USA. Am J Bot 88:667-676.

Richardson AD, Denny EG, Siccama TG, Lee X (2003) Evidence for a rising cloud ceiling in Eastern North America. J Climate 16:2093-2098.

Richardson AD, Lee X, Friedland AJ (2004) Microclimatology of treeline spruce-fir forests in mountains of the northeastern United States. Agric For Meteorol 125:53-66.

Richter BS, Benson DM, Ivors KL (2011) Microbial profiling of cultural systems for supression of *Phytophthora* root rot in Fraser fir. Plant Dis 95:537-546.

Robakowski P, Montpied P, Dreyer E (2002) Temperature response of photosynthesis of silver fir (*Abies alba* Mill.) seedlings. Ann For Sci 59:163-170.

Robakowski P, Montpied P, Dreyer E (2003) Plasticity of morphological and physiological traits in response to different levels of irradiance in seedlings of silver fir (*Abies alba* Mill). Trees 17:431-441.

Rossi S, Morin H, Deslauriers A, Plourde P (2011) Predicting xylem phenology in black spruce under climate warming. Global Change Biol 17:614-625.

Royce E, Barbour M (2001) Mediterranean climate effects. II. Conifer growth phenology across a Sierra Nevada ecotone. Am J Bot 88:919-932.

Sidor CG, Popa I, Vlad R, Cherubini P (2015) Different tree-ring responses of Norway Spruce to air temperature across an altitudinal gradient in the Eastern Carpathians (Romania). Trees 29:985-997.

Smith WK, Carter GA (1988) Shoot structural effects on needle temperatures and photosynthesis in conifers. Am J Bot 75:496-500.

Smith WK, Schoettle AW, Cui M (1991) Importance of the method of leaf area measurement to the interpretation of gas exchange of complex shoots. Tree Physiol 8:121-127.

Soulé PT (2011) Changing climate, atmospheric composition, and radial tree growth in a spruce-fir ecosystem on Grandfather Mountain, North Carolina. Natural Areas Journal 31:65-74.

Sprugel DG, Brooks JR, Hinkley TM (1996) Effects of light on shoot geometry and needle morphology in *Abies amabilis*. Tree Physiol 16:91-98.

Urban O, Janouš D, Acosta M, Czerný R, Marková I, Navrátil M, Pavelka M, Pokorný R, Šprtová M, Zhang R, Špunda V, Grace J, Marek MV (2007) Ecophysiological controls over the net ecosystem exchange of mountain spruce stand. Comparison of the response in direct vs. diffuse solar radiation. Glob Change Biol 13:157-168.

Varma V, Osuri AM (2013) Black Spot: a platform for automated and rapid estimation of leaf area from scanned images. Plant Ecol 214: 1529-1534

Vitasse Y, Hoch G, Randlin CF, Lenz A, Kollas C, Scheepens JF, Körner (2013) Elevational adaptation and plasticity in seedling phenology of temperate deciduous tree species. Oecologia 171:663-678.

Warren RJ, Bradford MA (2010) Seasonal climate trends, the north Atlantic osscillation, and salamander abundance in the Southern Appalachian Mountain region. J Appl Meteorol Climatol 49:1597-1603.

Wertin TM, McGuire MA, Teskey RO (2012) Effects of predicted future and current atmospheric temperature and [CO_2] and high and low soil moisture on gas exchange and growth of *Pinus taeda* seedlings at cool and warm sites in the species range. Tree Physiol 32:847-858.

Witkowski ETF, Lamont BB (1991) Leaf specific mass confounds leaf density and thickness. Oecologia 88:486-493.

Worrall J (1983) Temperature – bud-burst relationships in Amabilis and Subalpine fir provenance tests replicated at different elevations. Silvae Genetica 32:203-209.

Yamori W, Hikosaka K, Way DA (2014) Temperature response of photosynthesis in C_3, C_4, and CAM plants: temperature acclimation and temperature adaptation. Photosynth Res 119:101-117.

Zhang C, Tian H, Chappelka AH, Ren W, Chen H, Pan S, Liu M, Stylers DM, Chen G, Wang Y (2007) Impacts of climatic and atmospheric changes on carbon dynamics in the Great Smoky Mountains National Park. Environ Pollut 149:336-347.

Zhou Y, Wang C, Han S, Cheng Z, Li M, Fan A, Wang X (2011) Species-specific and needle age-related responses of photosynthesis in two *Pinus* species to long-term exposure to elevated CO_2 concentration. Trees 25:163-173.

Appendix

Table I. Description and images of phenological stages of bud-burst, provided by the North Carolina Cooperative Extension Service.

Description	Image	Description	Image
Stage 1 Dormant buds with thick waxy coats and blunt tips, ranging from white to dull shades of red, brown, and purple.		**Stage 5** Bud scales begin to separate at tips and turn white.	
Stage 2 Tips begin elongating, appearing wet and sticky. Base and sides still waxy and dull.		**Stage 6** Green shoots visible beneath white scales, but have not yet emerged.	
Stage 3 Base begins to swell. Waxy coats become shiny or translucent, and bud scales become darker brown.		**Stage 7** Complete bud-burst. Green shoots emerging.	
Stage 4 Tips elongate and become pointy, and become deep brown or red.			

Table II. Parameters of models used to calculate timing of bud-burst. General form: $y = a + (b-a)/(1+e^{(x0-x)/m})$.

Equation Coefficients	Low Elevations	Middle Elevations	High Elevations
a	0.60	1.15	0.83
b	7.11	7.24	7.12
x_0	119.56	125.98	124.32
m	5.66	5.30	6.13
r^2	0.9945	0.9897	0.9951

Table III. Parameters of models used to calculate timing of shoot expansion. General form: $y = a*x^b/(x_0^b + x^b)$.

Equation Coefficients	Low Elevations	Middle Elevations	High Elevations
a	12.09	12.90	12.44
b	22.90	19.48	19.88
x_0	144.63	152.46	151.08
r^2	0.9925	0.9863	0.9923

Table IV. Parameters of models used to calculate timing of trunk growth. General form: $y = a*x^b/(x_0^b + x^b)$.

Equation Coefficients	Low Elevations	Middle Elevations	High Elevations
a	7.57	11.47	8.10
b	6.73	5.79	6.90
x_0	204.61	196.32	181.12
r^2	0.9702	0.9714	0.9733

Vita

Scott Thomas Cory was born in 1991 in Lexington, North Carolina. He attended the University of North Carolina at Chapel Hill from 2009 to 2013. During his time at UNC, his interest in plant physiology began through coursework with Dr. Alan Weakley and Dr. Patricia Gensel. He was awarded a Bachelor of Science degree in Biology and a minor in Music in May 2013. Immediately after graduation, he worked as a technician for Dr. James S. Clark at the Nicholas School of the Environment at Duke University. From 2013 to 2015 Scott was a graduate student in the Department of Biology at Appalachian State University. Prior to graduation from ASU, he began doctoral work with Dr. William K. Smith at Wake Forest University.